

## THE STANFORD TWO-MILE LINEAR ACCELERATOR\*

R. B. Neal  
Stanford Linear Accelerator Center, Stanford University, Stanford, California

In April 1957, Stanford University proposed the construction of a two-mile-long linear electron accelerator capable of accelerating electrons to energies of 10 to 20 GeV for use in physics research. Congressional authorization for this machine was given in September 1961, and construction of the Stanford Linear Accelerator Center (SLAC) started in July 1962 on 480 acres of land near Stanford University under a prime contract with the U. S. Atomic Energy Commission.<sup>1</sup> The Center now includes more than a dozen large buildings and has a staff of approximately 1150 to operate and use the two-mile-long scientific instrument. Significant technical milestones during the construction period have been: Acceleration of an electron beam through the first two sectors (each sector 333 ft. long) on January 3, 1965; operation of 2/3 of the machine (6700 ft. ) on April 21, 1966. On May 21, 1966, approximately 4 years after start of construction, a beam was accelerated from an injector located at the west end through the entire two-mile length (30 sectors) into a "beam dump" located in the beam switchyard at the east extremity of the machine. During the first full length operation, an energy of 10 GeV was obtained with 24 of the 30 sectors contributing to the acceleration but operating at reduced power levels. In subsequent tests, the energy has been increased to 18.4 GeV but a full power run up to the 20 GeV design level has not yet been attempted.

(Submitted to Physics Today)

---

\* Work supported by U. S. Atomic Energy Commission

Further testing is continuing with the objective of starting the physics research program late in 1966. The experimental program and the basic apparatus which will be employed are described in a companion article ("The Initial Experimental Program of SLAC" by J. Ballam in this same issue).

The relative position of the SLAC machine in the international family of particle accelerators is shown in Fig. 1. Not noted on this graph but of interest is the fact that all of the proton machines shown accelerate their particles along approximately circular orbits. This is also true of the majority of the electron machines. But the four highest current electron accelerators (Orsay, Kharkov, Stanford, and SLAC) accelerate their electrons along a straight path. The existing Stanford machine referred to here is the 1.1 GeV Mark III accelerator which began operation in 1951. The largest and most energetic machines now in operation are the alternating gradient synchrotrons at the Brookhaven and CERN Laboratories each of which accelerates protons to about 30 GeV. They will be surpassed when the Russian 70 GeV machine at Serpukhov starts operations, probably in 1967. Two "super" energy circular proton accelerators of 200 and 800 GeV are under consideration at the Berkeley and Brookhaven Laboratories.

The two-mile Stanford accelerator is distinguished, not only by its length and high energy (Stage I, 20 GeV), but also by its high current, which exceeds that of any other machine of any kind now operating by an order of magnitude. Moreover, provisions have been made in the design of this machine which permit its later expansion (Stage II) to twice the energy (40 GeV) and twice the current (60  $\mu$ A) by connecting additional radiofrequency sources along its length. If desirable, the energy increase can be accomplished in step-wise manner.

## GENERAL DESCRIPTION

An air view of the SLAC site is shown in Fig. 2. This site is located about 2 miles west of the main University campus. The site is 1000 feet wide along most of the accelerator length. It increases to about 3000 feet at the target end to allow space for laboratories, shops, and experimental facilities.

A cross section of the underground 10-ft.  $\times$  11-ft. accelerator housing and the above-ground 13-ft.  $\times$  29-ft. klystron gallery is shown in Fig. 3. The two housings are separated by 25 feet of earth for radiation shielding. An interconnecting service shaft every 20 feet carries utilities, vacuum manifolds, instrumentation and control cables, and radiofrequency waveguides between the two levels. A personnel access way is provided once in each 333 ft. sector.

The beam switchyard located at the target (east) end of the accelerator is shown in Fig. 4. This large underground housing, approximately 1000 ft. long, contains the beam transport systems and instrumentation required to analyze and select the characteristics of the beam and to direct it into the various experimental areas.

Beyond the beam switchyard is the research area consisting of two large buildings and many smaller structures on about 20 acres of land. The larger of the buildings, having a floor area of 25,000 square feet and walls 70 feet high, will be used primarily for electron and positron scattering experiments and for photoproduction studies. The smaller building has an area of 17,000 square feet and will be the center of activity for experiments involving secondary particles.

A block diagram illustrating the principal components and systems of the accelerator is shown in Fig. 5. Most of these units are repeated many times in the entire accelerator length. For example, there are 960 ten-foot-long accelerator sections, 245 klystrons, 245 modulators, 30 sub-booster klystrons, 30 power sub-stations, 30 vacuum systems, etc. The instrumentation and control system is spread over the entire accelerator length, although the machine can be operated from a single Central Control Room.

A summary of the specifications of the two-mile accelerator is given in Table I.

#### Accelerator Structure

The accelerator proper is a cylindrical copper disk-loaded structure<sup>2</sup> in which an axial electric accelerating field is set up when the structure is excited with microwave power at a frequency of 2856 megacycles per second. The structure is designed to produce a constant axial electric field over the length of each independently-fed 10-ft. section. This constant gradient characteristic is achieved by suitable variation of the modular dimensions of the section. The shunt impedance of the structure is approximately 53 megohms per meter which results in an electron energy gain in MeV in a 10-ft. section of  $\approx 10 P^{\frac{1}{2}}$  where P is the input radiofrequency power to the section in megawatts.

The accelerator structure was fabricated by a brazing technique from the basic disk and ring elements shown in Fig. 6. These parts were independently machined to accuracies of  $\pm 0.0002$  inch. They were then carefully stacked and clamped together on a stainless steel mandrel passing through the disk apertures. Brazing was accomplished in a special flame furnace which provided a reducing atmosphere both inside and outside of the structure to prevent

oxidation. A completed 10-foot section is shown in Fig. 7.

Four of the 10-ft. sections are mounted on a 40-ft. aluminum girder, 24 inches in diameter, as shown in Fig. 8. This is the modular length of the accelerator for support and alignment purposes. The aluminum girder serves dual purposes as support for the accelerator and as a "light pipe" for alignment purposes (see below).

### Klystrons

The radiofrequency power sources are high power klystron amplifiers. A basic tube having a design capability of 24 megawatts peak and 22 kilowatts average power was developed at SLAC.<sup>3</sup> Four commercial companies also developed tubes meeting the same basic specification as the SLAC tube. A group photograph of the five different tubes is shown in Fig. 9. All of these tubes have permanent magnet focusing and are electrically and mechanically interchangeable.

The power from each klystron is divided four ways (Stage I) and is used to supply power to the four 10-ft. sections located on a single 40-foot girder. The general arrangement of the klystron, the connecting waveguides and the accelerator sections is shown in Fig. 10. Waveguide feeds to the accelerator connect to opposite sides of successive sections to compensate for deflecting forces due to residual coupler asymmetries. The provision of a waveguide valve just above each klystron allows the klystron to be replaced without affecting the accelerator vacuum or interfering with beam operation. If Stage II is later authorized, the number of klystrons will be increased to 960 so that each klystron will feed a single 10-ft. section.

### Drive and Phasing System

The klystron amplifiers must receive coherent low level signals at 2856 megacycles per second in order that the radiofrequency waves in the accelerator sections will have the correct frequency and phase relationships with the individual bunches of electrons passing through the accelerator. The rf drive system consists of (a) a master oscillator providing 476 Mc/sec power, (b) a main booster amplifier which increases the 476 Mc/sec power to 17.5 kw, continuous wave, (c) a 3-1/8-inch diameter main drive line two miles long, (d) couplers and varactor frequency multipliers at each 333-ft. sector which remove a small portion of the main drive signal and multiply the frequency by 6 to 2856 Mc/sec, (e) a pulsed sub-booster klystron at each sector which amplifies the 2856 Mc/sec power by 60 dB, (f) a 1-5/8-inch diameter coaxial line which transmits 2856 Mc/sec drive power to the vicinity of each of the high power klystrons in the sector, and (g) couplers which remove approximately 300 watts peak to drive each klystron.

The main drive signal is transmitted at the sub-harmonic frequency, 476 Mc/sec, since the low loss at this frequency ( $\approx 0.25$  dB/100 ft.) permits transmission over two miles without series boosters which, if used, would lead to phase shift and reliability problems.

The rf phasing system<sup>4</sup> uses the phase of the electron bunches in the accelerator as the phase reference. It is based on the principle that the wave induced by the bunched electron beam in an accelerator section is  $180^{\circ}$  out of phase with respect to the wave from a correctly phased klystron supplying power to the section. Phasing is accomplished automatically (within  $\pm 5^{\circ}$ ) by sectors at the initiation of the operator.

## High Power Modulators

Each klystron amplifier is provided with a "line-type" modulator<sup>1(c)</sup> rated at 65 megawatts peak and 75 kilowatts average power, a pulse length of 2.5 microseconds, and a maximum pulse repetition rate of 360 pps. The pulse-forming network in the modulator is discharged through a single hydrogen thyatron capable of handling the entire peak and average power requirements. The voltage of the output pulses from the modulator is increased by a factor of 12 by means of a pulse transformer, and the resulting pulses at a voltage of 250 kV (maximum) are then applied to the associated klystron.

Each modulator is provided with a de-Q'ing circuit which compares the charging voltage of the pulse network during each charging cycle to a reference voltage. When the level of the charging voltage reaches the reference level, the energy stored in a charging transactor is dumped into a dissipative circuit by means of a silicon-controlled rectifier switch. This effectively clamps the charging voltage at the reference level and thus stabilizes the output pulses from the modulator to  $\pm 0.1\%$  even in the presence of significant ( $\approx \pm 5\%$ ) variations in the ac line voltage.

## Injector System

A diagram of the main injector<sup>5</sup> is shown in Fig. 11. It is designed to inject a well bunched ( $5^0$ ) and well collimated beam of electrons into the accelerator. Since the energy gain of an accelerated electron is proportional to the cosine of the phase angle it occupies with respect to the peak of the traveling radiofrequency wave, good bunching of the electrons is essential in order to attain a narrow electron energy spectrum at the output of the accelerator. The electron gun which operates at 80 kV is of the triode type which permits the pulse length and beam current to be selected on a pulse-to-pulse basis

from any of three predetermined sets of values. This feature of the injector, together with the ability to trigger the klystrons in the various sectors in time with or after the beam (or at various repetition rates), permits carrying on several simultaneous experiments in the research areas at different incident energies, pulse lengths, and intensities. The pre-buncher consists of a velocity modulation cavity. The bunching section is a disk-loaded section 10-cm long in which the phase velocity is 0.75 c. It serves to reduce the phase spread by a factor of 2 (while doubling the momentum spread) and increases the beam energy to 250 kV. A 10-foot long constant gradient accelerator section increases the energy to approximately 30 MeV. For phase synchronization, the pre-buncher, buncher, and 10-foot accelerator section are all driven by power from the same klystron, which is conservatively run at 1/2 to 2/3 of its power capability to give good life stability.

#### Positron Source

A positron beam is desired at the 2/3 point along the accelerator length for injection into a proposed positron-electron storage ring<sup>6</sup> and at the main experimental station at the end of the accelerator for positron scattering experiments. The positron beam is created at the 1/3 point along the machine by inserting a converter and reversing the rf phase of the first 1/3 of the accelerator. With 100 kW of incident electron beam power, it is predicted that approximately  $2.5 \times 10^{10}$  positrons per pulse can be accelerated in an energy band of about 1% and a transverse phase space of approximately 0.15 (MeV/c) (cm).

The positron source system is shown in Fig. 12. Either of two separate radiators can be inserted into the beam. A radiator has a thickness of about 3.5 radiation lengths and consists of one layer of gold, two of silver, and



eight of copper with cooling water passages between. Each layer is approximately 1/8-inch thick. A "wand" radiator is provided for intermittent positron pulses at rates of one per second or less. It is a small target about 0.5-inch wide driven across the beam line on command in a time equivalent to about 5 machine pulses (at 360 pps). The center pulse of this group results in a positron pulse; the other 4 are caused to be blank by gating the main injector. All other pulses may be the electron beam, if desired. The second radiator is in the form of a rotating water-cooled wheel. It is used when continuous positron production is desired.

A magnetic lens system is used to improve the match between the source emittance and the accelerator phase space acceptance. The radiator is located in a 20-kG axial magnetic field which decreases rapidly to 2.4-kG about 2 feet downstream of the radiator and then remains constant for the next 25 feet. Acceleration begins 2.5-feet downstream of the radiator and the positron energy at 25 feet is about 75 MeV, at which point the solenoidal focusing is replaced by a series of 13 quadrupole triplets whose spacing increases with energy until this focusing system merges with the regular machine triplet system located at the end of each sector.

A pulsed rf deflector located downstream of the converter is used to produce an angular deflection of the positron and electron beams. Since the beams are  $180^\circ$  apart in phase, they are both deflected by the same angle; depending on which beam is needed, a magnetic dipole can then be used to restore the direction of either the positron or the electron beam to the axis while deflecting the other even farther.

## Beam Guidance and Diagnostic Equipment

To compensate for the earth's magnetic field and for stray ac and dc fields along the machine, parallel degaussing wires and concentric magnetic shielding are provided, reducing the average fields to  $< 10^{-4}$  gauss.<sup>7</sup> The degaussing currents are independently adjustable for each sector. The magnetic shielding material consists of 0.006-inch of moly-permalloy material which results in a local shielding factor of about 30 and an overall effective value of about 10, considering unavoidable gaps.

Beam monitoring, steering, and focusing devices are provided in a 10-foot drift section at the end of each 333-foot sector of the accelerator. The layout of a standard drift section is shown in Fig. 13. Equipment in this section consists of a quadrupole triplet, steering dipoles (X and Y), a phase reference cavity, beam position monitors (X and Y), a beam intensity monitor, a beam profile monitor, and a "beam scraper" (collimator). The beam position monitors consist of two rectangular cavities which are excited in the  $TM_{120}$  mode by an off-axis beam. Since the phase of the excitation depends on the direction of beam deviation from the axis, the sense of the deviation can be detected by comparing the phase of the wave from the beam position monitor cavities with the phase of the wave from the phase reference cavity which is excited in the  $TM_{010}$  mode. Beam positions accurate to  $< 1.0$  mm from 30 such systems are presented at Central Control.

## Trigger System

Although the basic repetition rate of the accelerator is 360 pps, the trigger system permits operation of various accelerator sectors and other subsystems in a very flexible manner so that up to six beams having distinct energies, currents, and destinations in the research area can be programmed.

The repetition rates of these beams can be adjusted to be any value between 1 and 360-pps. The trigger system is illustrated in Fig. 14. Clock pulses at 400-volt level and 360 pps are sent over the entire two-mile length along a single 1-5/8-inch diameter coaxial cable. A small amount of power is removed from the main line by means of couplers at each station (injector, accelerator section, positron source, etc.) and is sent to the local trigger generator. A gating pulse is sent to each local trigger generator from the pattern generator in Central Control. Since the timing precision ( $\approx 25$  nanoseconds) is inherent in the clock pulses, the gating pulses do not have to be very precise and can be transmitted on ordinary wire pairs.

In Fig. 14, the pattern generator pulses are shown gating the clock pulses admitted to the klystron modulators of each sector. If a particular sector is not to contribute to the energy of a particular beam, the pattern gating signal causes the modulators to be triggered approximately 25 microseconds late, after the beam pulse has been transmitted through the sector. In other arrangements, the pattern signals may cause a particular sector to pulse at lower repetition rates, such as 60, 120, and 180 pps.

#### Vacuum System

The all-metal high vacuum system<sup>8,9</sup> capable of maintaining the accelerator and waveguides at  $<10^{-6}$  torr is shown schematically in Fig. 15. One such system is provided for each 333-foot sector. Four 500-liter/second getter-ion pumps located in the Klystron Gallery evacuate the accelerator and waveguides through interconnecting stainless steel manifolds. A pump can be removed for servicing without interference with accelerator operations by closing the associated 6-inch valve. Similarly, an individual klystron can be replaced by closing the 3-inch valve connecting it to the pumping manifold and the waveguide vacuum valve in its output rf system.

Separate pumping systems are provided for rough-pumping the accelerator, for the 24-inch "light pipe", and for the Beam Switchyard.

#### Alignment System<sup>10</sup>

Each of the 40-foot support points of the accelerator is aligned with respect to a straight line defined by two end points. One of the end points is a laser light source located at the end of the accelerator near the Beam Switchyard and the other end point is a slit with a photomultiplier detector located upstream from the main injector. The laser light source provides a beam of light which is transmitted through the 24-inch aluminum support girder. The girder ("light pipe") is evacuated to a pressure of about 10 microns to reduce refraction due to temperature gradients in the residual gas. At each 40-foot support point, a retractable Fresnel target, as shown in Fig. 16, images the light source on the detector. The transverse location of the image indicates the deviation of the target from its correct position. The adjustable jacks at the corresponding support point can be adjusted to bring the target into correct alignment. The correct angular rotation of the accelerator is assured by the use of precision level devices. The system described is able to align the accelerator to  $\pm 0.5$  mm.

#### Beam Switchyard<sup>11</sup>

A layout of the Beam Switchyard is shown in Fig. 4. This is a large two-level underground structure located under 40 feet of concrete and earth for radiation shielding purposes. The beam path itself is located on the lower level. The upper level contains utility runs, instrumentation and control alcoves, cranes, service cars, and other equipment required in conjunction with the main beam handling equipment in the lower level.

By the use of a pulsed deflecting system which deflects the electrons (or positrons) on a pulse-to-pulse basis into any of 3 large dc magnet transport

systems-it is possible to carry out several experiments simultaneously in the research area using time-interlaced beams.

The unusually high power ( $\approx 1$  MW in Stage I) carried by the incident beam has imposed very difficult problems in the design of the beam handling equipment. A typical example of a device capable of handling these large beam powers is the 16-foot-long adjustable energy-defining aluminum slit<sup>12</sup> shown in Fig. 17. Two in-line slits of the type shown, with the second rotated  $90^\circ$  about its axis with respect to the first, are used as an adjustable collimator at the beginning of the Beam Switchyard.

A small digital process control computer (CDC 925) will be used in the control system of the Beam Switchyard. This computer will read data from punched cards and send control information to the regulators in the magnet power supplies where a digital-to-analog converter will convert the digital information to an analog reference voltage. Slits and collimators will be adjusted in a similar way. When desired by the operator or experimentalist, data representing the parameters of a particular beam will be printed out from the computer memory for record, together with auxiliary information. About 100 signals from various sources will be scanned every accelerator pulse (1/360 second) and about 600 signals will be scanned at a slower rate. The computer will detect, identify, and print out the time and date of any changes in the interlock and status signals in proper sequence.

## OPERATING RESULTS

Tests to date have confirmed the principal design parameters of the accelerator.

### Energy Gain

The basic equation for energy gain in a multiple-feed linear accelerator of constant gradient design is:

$$V = \left(1 - e^{-2\tau}\right)^{\frac{1}{2}} \sum_N \left(P_n \ell r\right)^{\frac{1}{2}} - \frac{i r N \ell}{2} \left(1 - \frac{2\tau e^{-2\tau}}{1 - e^{-2\tau}}\right)$$

where

- N = Number of independently fed sections
- $\ell$  = Length of each section
- $P_n$  = Input rf power to section n
- r = Shunt impedance per unit length
- i = Peak beam current
- $\tau$  = Rf attenuation in accelerator section in nepers

The first term in this equation is the "no-load" energy, i. e. , the energy obtained with negligible beam current. The second term is the correction for beam loading; it is directly proportional to the beam current. Using the design parameters of the SLAC accelerator ( $N = 960$ ,  $\ell = 3.05$  meters,  $r = 53$  megohms/meter, and  $\tau = 0.57$  nepers) and taking into account the fact that each klystron feeds its power equally into 4 accelerator sections and that some of the power ( $0.54 \pm 0.1$  dB) is dissipated in the waveguides connecting the klystrons to the accelerator, the above equation becomes:

$$V_{\text{GeV}} = 0.020 \sum \left(P_{\text{MW}}\right)^{\frac{1}{2}} - 0.035 i_{\text{mA}}$$

For example, this equation states that if each of the 245 klystrons connected to the accelerator is producing 16 megawatts, each klystron and its 4 associated 10-foot sections would contribute an electron energy gain of 80 MeV and the total no-load energy in the two-mile accelerator (assuming perfect phasing) would be 19.6 GeV. Further, if the electron beam current were 20 mA, the resulting beam loading would reduce the energy by 0.70 GeV to 18.9 GeV. The coefficients in the above equation have been verified within experimental accuracy (about 2%).

### Energy Spectra

Typical energy spectra are shown in Fig. 18. The spectrum of higher energy was obtained for light beam loading (2.3 mA peak beam current). A higher beam current (15 mA) results in the lower energy spectrum having 0.44 GeV less energy than the first. Note that the lower energy spectrum contains some electrons having energies as high as the lightly loaded spectrum. These are the electrons which pass through the accelerator during the earliest part of the pulse before a significant amount of stored rf energy has been absorbed by the beam. The spectrum width at half maximum is 1.33% of which about 0.9% is attributable to the resolution of the measurement devices.

The broadening of the energy spectrum with increasing beam loading as shown in Fig. 18 is undesirable in many research applications. Compensation for beam loading can be achieved by delaying the trigger to one or more of the accelerator sectors. In this case, the first electrons accelerated during the beam pulse pass through some sectors which are only partly filled with rf energy and therefore they gain less energy than they would if the sectors were completely filled. The compensation achievable with this technique is

demonstrated in Fig. 19 where the dashed line shows the uncompensated spectrum and the solid line shows the compensated spectrum resulting from trigger delay to one sector by approximately 0.5 microseconds.

### Electron Bunching

Beam dynamics studies have shown that the electron bunch length at the 30-foot point along the accelerator corresponds to  $\approx 5^\circ$  (1/72 of the operating wavelength of 10.5 cm ). A well-bunched beam is an essential factor in obtaining a good energy spectrum since the fractional energy spread,  $\delta V/V$ , resulting from a bunching angle of  $\alpha$  radians is  $\alpha^2/8$ . Thus,  $\delta V/V$  from this cause amounts to only 0.1% in the two-mile machine.

### Phasing

The accuracy to which the rf sources (klystrons) are phased influences how closely the maximum energy performance level can be approached. The fractional energy deviation from imperfect phasing is  $1/2 \overline{\theta^2}$  where  $\overline{\theta^2}$  is the average value of the square of the phasing error for the entire complement of klystrons. Measurements have shown that the automatic phasing system which uses the electron beam as a phase reference can achieve a  $\overline{\theta^2}$  of less than 0.01 ( $\theta \leq 5^\circ$ ). The resulting energy spread from phasing errors is therefore less than 0.5%.

### Beam Transmission

Beam transmission through the accelerator has been found to be quite good. About 90% of the current measured close to the input end of the machine, say 40 feet from the injector, is preserved through the entire two-mile length. This favorable result arises from the effective performance of the beam position and intensity monitors, the steering and focusing systems and the long ion



chamber. The microwave position monitors located at the end of each sector have been able to indicate the transverse position of the beam with respect to the accelerator axis within  $\pm 0.5$  mm. The long ion chamber, which is an argon-filled coaxial line installed along-side the operator to detect beam losses and from the times of arrival of the ionization signals to resolve their location within one to two hundred feet.

The transverse phase space of the beam is an index of its "optical" quality and of its suitability as a research tool. The phase space is given approximately by the product of the beam diameter at the beam minimum times the angular divergence of the beam. At about 40 feet downstream from the injector, 80% of the injected beam current is found in a phase space of  $1.2 \times 10^{-2}$  (MeV/c) (cm) (expressed as a product integral of the transverse momentum in units of MeV/c and the beam displacement in cm). A second measurement at the beam switchyard beyond the accelerator indicates that the same fraction of the beam is contained in a phase space of about  $3 \times 10^{-2}$  (MeV/c) (cm). Since the beam diameter is approximately 0.4 cm at this point, the angular divergence at an energy of 10 to 20 GeV is less than  $10^{-5}$  radians. Thus, the natural increase in the transverse dimensions of the beam in passing through the entire 1000 foot beam switchyard enroute to the research area is no more than 0.1 inches. The beam "spot" observed at the end of the accelerator is shown in Fig. 20.

As mentioned earlier, the ability to accelerate multiple time-interlaced beams is very important in that it permits simultaneous physics experiments to be carried out in several physically separated areas. Tests to date have demonstrated the feasibility of accelerating at least three beams of different energies simultaneously. The pulse length and intensity of each of these beams can be independently controlled.

## Beam Break-up

During initial operation of the machine a phenomenon called "beam break-up" has been encountered. This difficulty, observed in earlier accelerators,<sup>13</sup> manifests itself as a progressive shortening of the electron beam pulse length as the beam current is increased. Design steps (such as employment of the constant gradient accelerator structure) which were taken in the two-mile machine to combat this phenomenon appear to have alleviated but not to have cured the problem. The attainable intensity is at present limited to about one-half the design value of 30 microamperes average beam current (50 milliamperes peak current at 360 pulses per second). Corrective measures are being investigated both theoretically and experimentally even though the achievable current is adequate for all experiments now planned or contemplated.

Beam break-up in the two-mile accelerator is attributed to the transverse fields arising from the excitation by the beam of a higher order  $TM_{11}$ -like mode in each 10-foot accelerator section. This occurs at a frequency of  $\approx 4140$  megacycles per second although other frequencies (such as 1284, 1572, 4428, etc.) resulting from beating of 4140 with the various harmonics of 2856 Mc/sec are also observable as modulation of the electron beam. The 4140 Mc/sec frequency originates as a resonance in the first 8 to 10 cavities of each 10-foot accelerator section. There are several other near-by resonances involving other groups of cavities in the structures but they are weaker than the 4140 Mc/sec resonance which seems to be principally responsible for beam break-up. In a multiple section machine, the beam interacts successively with the excited region of each section. The resulting transverse modulation of the beam causes an even higher excitation of succeeding sections. In a given section the later arriving electron bunches during a pulse add to the already existing excitation. Thus, the build-up of the

transverse deflecting mode increases both with time and with distance down the machine. Alternate electron bunches are deflected to opposite sides. Beam break-up occurs at a time and at the position along the accelerator where the amplitude of the transverse displacement equals the aperture of the accelerator. However, even at a given beam current, the time and position of beam break-up are not unique. When break-up occurs the beam current first strikes the walls of the accelerator at the end of the machine. Then, the continuously expanding displacement causes later regions of the injected beam pulse to strike the walls progressively closer to the injection end of the machine. Theoretical considerations and experimental results indicate that beam break-up in a given accelerator structure can be characterized by the simple expression

$$\frac{it_p z}{\partial V/\partial z} = K$$

where  $i$  is the peak beam current at which blow-up occurs,  $t_p$  is the length of the beam pulse as limited by break-up,  $z$  is the distance from the injector to the closest position where current is lost at a time  $t$  during the beam pulse, and  $\partial V/\partial z$  is the average energy gradient in the accelerator. With  $i$ ,  $t$ ,  $z$ , and  $\partial V/\partial z$  expressed in units of milliamperes, microseconds, feet, and MeV/ft, respectively, the value of  $K$  in the SLAC accelerator has been found to be approximately  $2 \times 10^5$ . For example, at an energy of 16 GeV ( $\partial V/\partial z = 1.6$  MeV/ft.), the threshold current for beam break-up at a pulse length of 1.6 microseconds is about 20 mA for the entire 10,000 ft. accelerator. At 40 mA the pulse length for the entire machine shortens to about 0.8 microseconds. On the other hand, a peak current of 40 mA can exist for the entire 1.6 microseconds over the first 5000 ft. of the machine.

It has been observed that as the current is increased, beam break-up first occurs in a vertical orientation in the accelerator. This is believed due to the fact that the waveguide feed orientation is horizontal, partially suppressing the horizontally oriented transverse mode. As the beam current is increased further, beam break-up occurs randomly in both the horizontal and vertical planes. The threshold current for horizontal break-up is about 1-1/2 times the threshold value for vertical break-up.

Various means of curing or alleviating the beam break-up problem are under investigation. These include microwave suppression and feed-back schemes, the addition of sextupole or octupole devices, and improved quadrupole focusing along the machine. The latter measure is the only one which has thus far been found to be definitely efficacious. The improvement in beam break-up threshold which can be obtained with stronger quadrupole focusing is shown in Fig. 21. The quadrupoles used are the triplets at the end of each 333-ft. sector. Effective quadrupole strength is given in terms of the parameter  $l/\lambda_t$  where  $l$  is the length of 1 sector (333 ft.) and  $\lambda_t$  is the focusing wavelength. The symbol  $I_Q$  denotes the maximum value of quadrupole current used at any point in the machine. The current in the quadrupoles increases linearly sector by sector up to the value of  $I_Q$  at sector 30. By increasing the quadrupole current capacity (or the number of quadrupoles) beyond the present capacity it appears possible to raise the beam break-up current threshold significantly. Present plans are to rearrange the individual quadrupoles of the existing sets of triplets in the form of doublets. The shorter quadrupoles will be used as doublets in the early part of the accelerator and the longer quads as doublets in the down-stream sectors of the accelerator. Larger power supplies will be provided for the down-stream doublets. At a somewhat later date additional singlet quadrupoles will be added at 40-foot intervals in the first few sectors of the accelerator. These steps are expected to increase the beam break-up threshold to the design current level or higher.

## Endurance Test Results

Since the replacement of the klystron amplifiers is one of the major cost factors in the operation of the two-mile accelerator, efforts have been made to obtain valid predictions of these costs in advance of undertaking the initial research program. Endurance tests involving 14 sectors (112 klystrons) have been run under 7 different operating conditions as noted in Table II. The variables were the pulse repetition rate which ranged from 60 to 360 pulses per second and the klystron beam voltage ranging from 200 to 245 kV. The corresponding peak power outputs and the equivalent electron beam energies (assuming 230 klystrons in operation) are also given. Experimental results are the total failures under each condition in approximately 1200 hours of operation and the average number of klystron station faults per minute (extrapolated to 230 stations). The number of failures for the various conditions ranged from 0 to 6 and the fault rate from 0.2 to 2.0 per minute. When a klystron station faults, the operator at present manually restores the tube to the operating condition. At a somewhat later date, a special circuit will be added in the machine control system which will automatically replace a faulting klystron with one from a small group kept on "stand-by" for this purpose.

## REFERENCES

1. For details of design evolution of the two-mile accelerator, see, for example:
  - (a) R. B. Neal and W.K.H. Panofsky, Proceedings of the International Conference on High Energy Accelerators (CERN, Geneva, 1956), Vol. I, p. 530.
  - (b) R. B. Neal, Proceedings of the International Conference on High Energy Accelerators (CERN, Geneva, 1959), p. 349.
  - (c) K. L. Brown, A. L. Eldredge, R.H. Helm, J.H. Jasberg, J. V. Lebacqz, G. A. Loew, R. F. Mozley, R. B. Neal, W.K.H. Panofsky, T. F. Turner, Proceedings of International Conference on High Energy Accelerators (Brookhaven, 1961), p. 79.
  - (d) W.K.H. Panofsky, Proceedings of the International Conference on High Energy Accelerators (Dubna, 1963), p. 407.
  - (e) J. Ballam, G. A. Loew, R. B. Neal, Proceedings of the Fifth International Conference on High Energy Accelerators (Frascati, 1965).  
(To be published.)
2. R. P. Borghi, A. L. Eldredge, G. A. Loew, and R. B. Neal, "Design and Fabrication of the Accelerating Structure for the Stanford Two-Mile Accelerator," Advances in Microwaves, Vol. I (Academic Press, New York, N. Y.).
3. J. V. Lebacqz, The First National Particle Accelerator Conference (Washington, D. C. , 1965), -IEEE Trans. Nucl. Sci. NS-12 (No. 3), 86 (1965).
4. C. B. Williams, A.R. Wilmunder, J. Dobson, H. A. Hogg, M. J. Lee and G. A. Loew, Proceedings of the G-MIT Symposium (IEEE), (Clearwater, Florida, 1965), p. 233.
5. R. H. Miller, R. F. Koontz, and D. D. Tsang, The First National Particle Accelerator Conference (Washington, D. C. , 1965), IEEE Trans. Nucl. Sci. NS-12 (No. 3), 804 (1965).

6. M. Allen, et al. , "Proposal for a High-Energy Electron-Positron Colliding-Beam Storage Ring at the Stanford Linear Accelerator Center," Stanford Linear Accelerator Center, Stanford, California.(Revised Sept. 1966.)
7. W. B. Herrmannsfeldt, The First National Particle Accelerator Conference (Washington, D. C. , 1965), IEEE Trans. Nucl. Sci. NS-12 (No. 3), 929(1965).
8. R. B. Neal, J. Vac. Sci. and Technol. 2 , 149 - 159 (1965).
9. S. R. Conviser, The First National Particle Accelerator Conference (Washington, D. C. , 1965), IEEE Trans. Nucl. Sci. NS-12 (No. 3), 699 (1965).
10. W. R. Herrmannsfeldt, The First National Particle Accelerator Conference (Washington, D. C. , 1965), IEEE Trans. Nucl. Sci. NS-12 (No. 3), 9 (1965).
11. R. E. Taylor, The First National Particle Accelerator Conference, (Washington, D. C. , 1965), IEEE Trans. Nucl. Sci. NS-12 (No. 3), 846 (1965).
12. D. R. Walz, J. Jurow, and E. L. Garwin, The First National Particle Accelerator Conference (Washington, D. C. , 1965), IEEE Trans. Nucl. Sci. NS-12 (No. 3), 867 (1965).
13. See, e. g. , T. R. Jarvis, G. Saxon, and M. C. Crowley-Milling, Proc. IEE 112, 1795 (1965).

TABLE I  
GENERAL ACCELERATOR SPECIFICATIONS

|                                   | STAGE I   | STAGE II             |
|-----------------------------------|---|----------------------|
| Accelerator length                | 10,000 feet   | 10,000 feet          |
| Length between feeds              | 10 feet   | 10 feet              |
| Number of accelerator sections    | 960   | 960                  |
| Number of klystrons               | 245   | 960                  |
| Peak power per klystron           | 6 - 24 MW   | 6 - 24 MW            |
| Beam pulse repetition rate        | 1 - 360 pps   | 1 - 360 pps          |
| RF pulse length                   | 2.5 $\mu$ sec   | 2.5 $\mu$ sec        |
| Filling time                      | 0.83 $\mu$ sec  | 0.83 $\mu$ sec       |
| Electron energy, unloaded         | 11.1 - 22.2 GeV   | 22.2 - 44.4 GeV      |
| Electron energy, loaded           | 10 - 20 GeV   | 20 - 40 GeV          |
| Electron peak beam current        | 25 - 50 mA  | 50 - 100 mA          |
| Electron average beam current     | 15 - 30 $\mu$ A   | 30 - 60 $\mu$ A      |
| Electron average beam power       | 0.15 - 0.6 MW   | 0.6 - 2.4 MW         |
| Electron beam pulse length        | 0.01 - 2.1 $\mu$ sec  | 0.01 - 2.1 $\mu$ sec |
| Electron beam energy spread (max) | $\pm$ 0.5%  | $\pm$ 0.5%           |
| Positron Energy                   | 7.4 - 14.8 GeV  | 14.8 - 29.6 GeV      |
| Positron average beam current*    | 1.5 $\mu$ A   | 1.5 $\mu$ A          |
| Multiple beam capability          | 3 interlaced beams with independently adjustable pulse length and current |                      |
| Operating frequency               | 2856 Mc/sec   | 2856 Mc/sec          |

\* For 100 kW of incident electron beam power at positron source located at 1/3 point along accelerator length.

Slide 603

m 711D-111



TABLE II  
ENDURANCE RUN

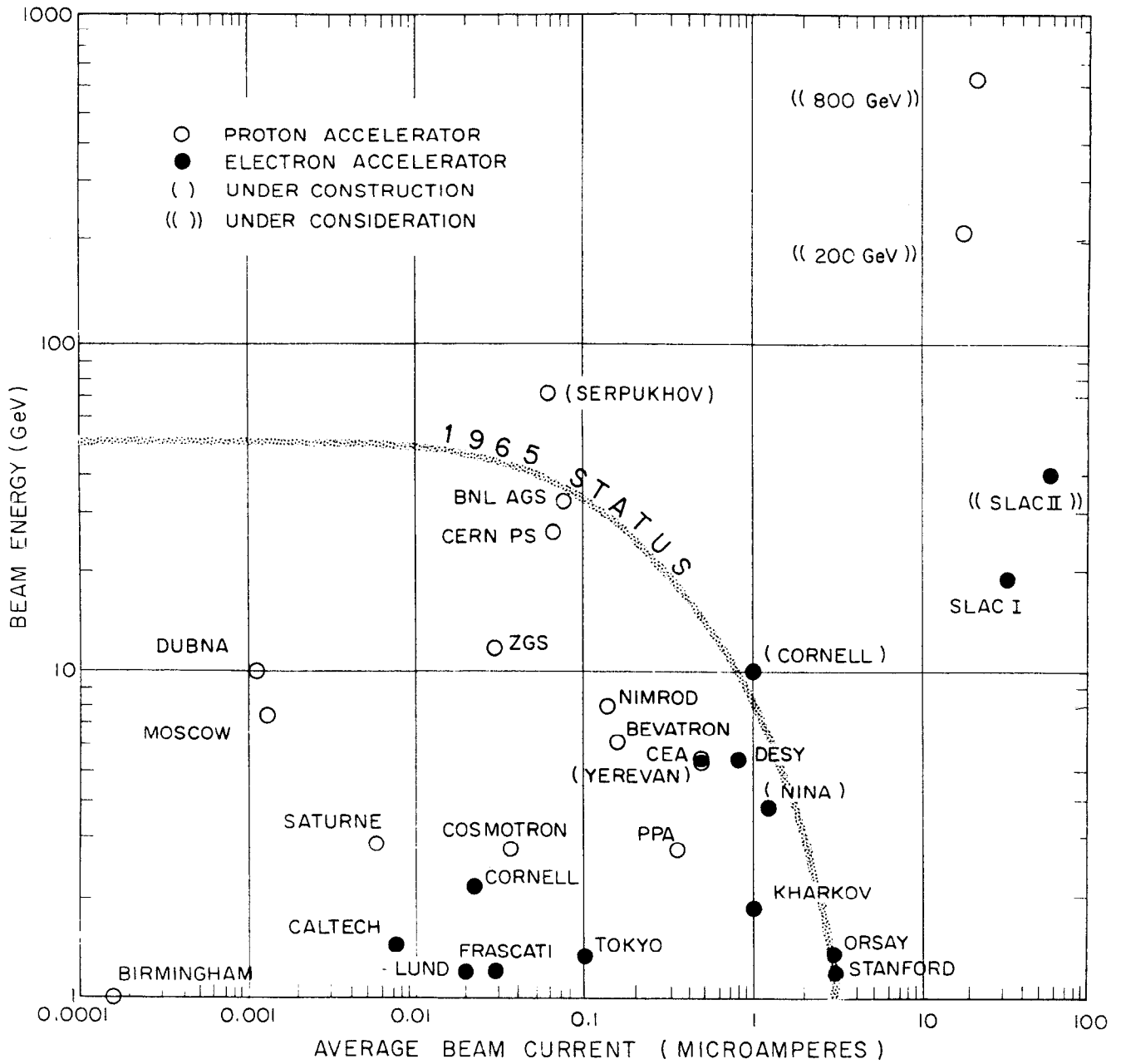
| SECTOR PAIR | OPERATING LEVEL        |                          |                         |              | ACCUMULATED HRS.<br>(Avg. of 16 Stations) | TOTAL KLYSTRON FAILURES | FAULTS PER MINUTE<br>(Extrapolated to 230 Stations) |
|-------------|------------------------|--------------------------|-------------------------|--------------|---|-------------------------|---|
|             | V <sub>K</sub><br>(kV) | P <sub>out</sub><br>(MW) | V <sub>o</sub><br>(GeV) | PRR<br>(pps) |   |                         |   |
| 3 & 4       | 245                    | 21                       | 21                      | 60           | 1175                                      | 1                       | 0.4   |
| 5 & 6       | 245                    | 21                       | 21                      | 360          | 1050                                      | 6                       | 2.0   |
| 7 & 8       | 230                    | 17.5                     | 19                      | 60           | 1200                                      |                         | 0.2   |
| 9 & 10      | 230                    | 17.5                     | 19                      | 180          | 1140                                      |                         | 0.2   |
| 13 & 14     | 230                    | 17.5                     | 19                      | 360          | 1135                                      | 2                       | 0.6   |
| 15 & 16     | 200                    | 12                       | 16                      | 60           | 1200                                      | 1                       | 0.2   |
| 17 & 18     | 200                    | 12                       | 16                      | 360          | 1190                                      |                         | 0.4   |

P<sub>out</sub> = Expected Average Power Output at Klystron  
- Beam Voltage V<sub>K</sub>

V<sub>o</sub> = Computed No-Load Electron Beam Energy for  
230 Stations Operating at V<sub>K</sub> (V<sub>o</sub> = 4.6√P<sub>out</sub>)

## LIST OF FIGURES

1. Comparative graph of various accelerators.
2. Air view of SLAC site showing the two-mile accelerator, the research facilities and the principal laboratories and shops.
3. Cross-section of accelerator housing and klystron gallery.
4. Beam switchyard plan.
5. Principal components and systems of accelerator.
6. Accelerator disks and cylinders.
7. View of completed 10-foot accelerator section.
8. Basic 40-foot accelerator module consisting of four 10-foot sections mounted on a 24-inch diameter aluminum girder.
9. Klystron models manufactured by SLAC and by four commercial companies. All these tubes are electrically and mechanically interchangeable.
10. General arrangement of klystron, connecting waveguides and four 10-foot accelerator sections.
11. Profile view of injector.
12. Positron source and its associated focusing and instrumentation equipment.
13. Standard instrument section located at end of each 333-foot sector.
14. Trigger system block diagram.
15. Vacuum system schematic for one 33-foot sector.
16. End of 40-foot girder showing retractable Fresnel target.
17. High-power energy defining slits located in beam switchyard.
18. Energy spectra under different beam loading conditions.
19. Compensation of spectrum broadening due to beam loading by trigger delay to 1 sector.
20. Beam spot observed at end of accelerator.
21. Threshold beam break-up current versus quadrupole focusing along accelerator. Quadrupole strength is given in terms of effective focusing wavelength.



NOV.'65, 157-1-A

FIG. 1

*Handwritten notes:*  
 DUBNA  
 MOSCOW

*Handwritten notes:*  
 M 21 10 65



FIG. 2

631-4-A

11/17/51  
S  
3/11

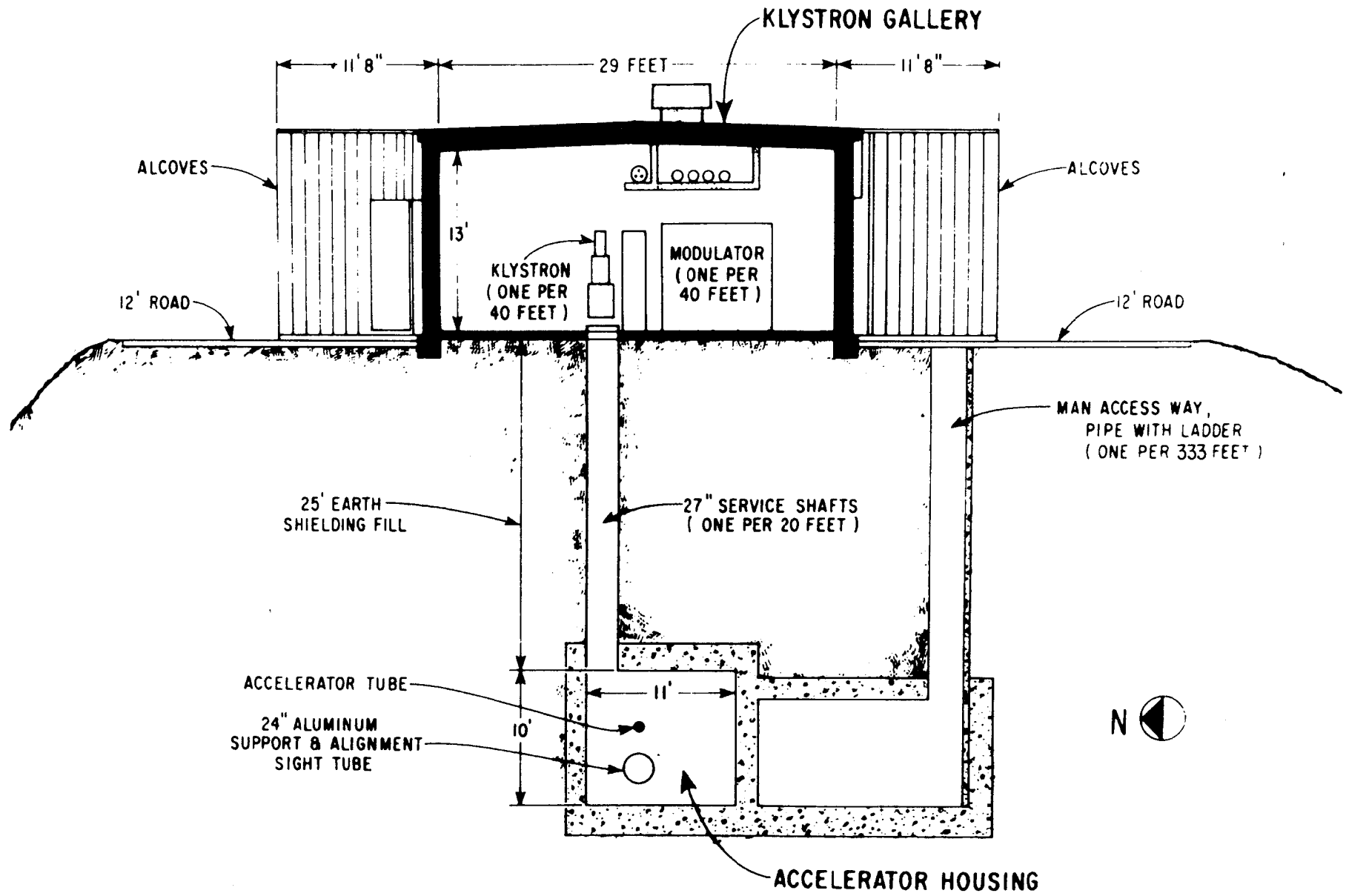
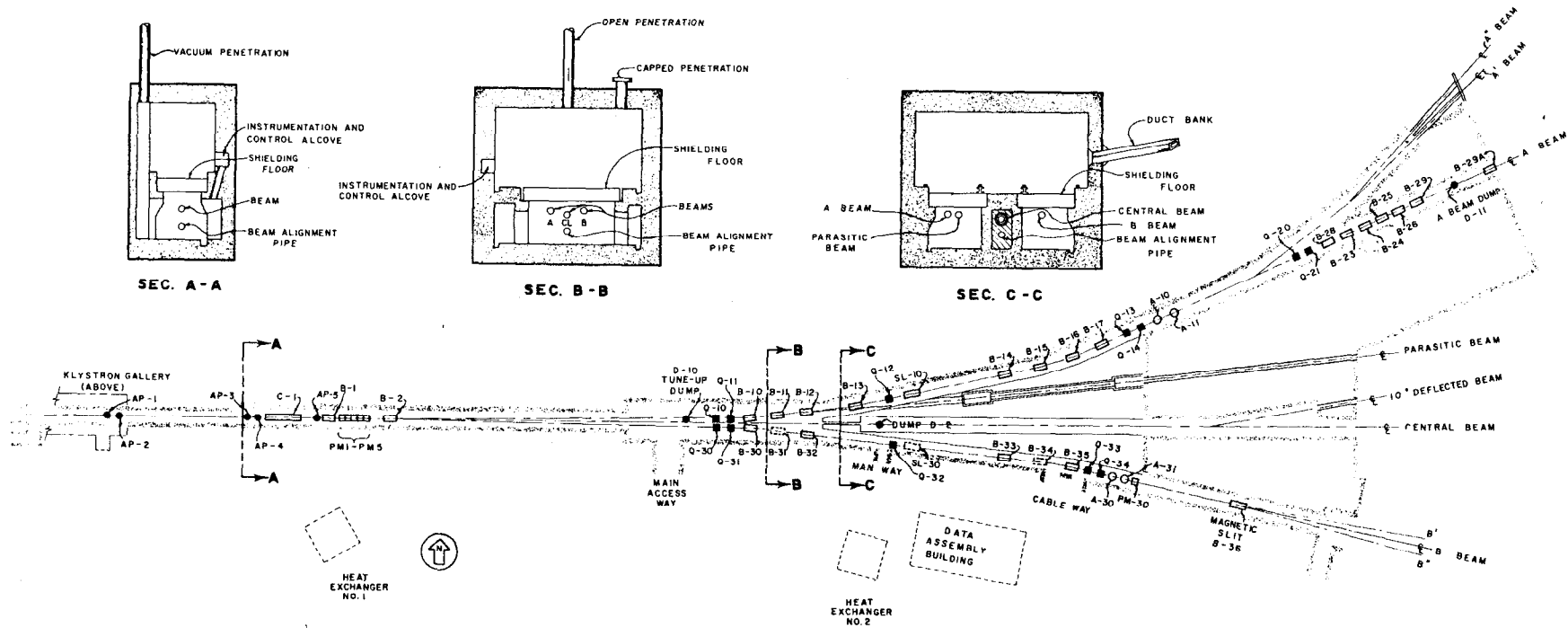


FIG. 3

*M 2094 /  
also M 1863-4*

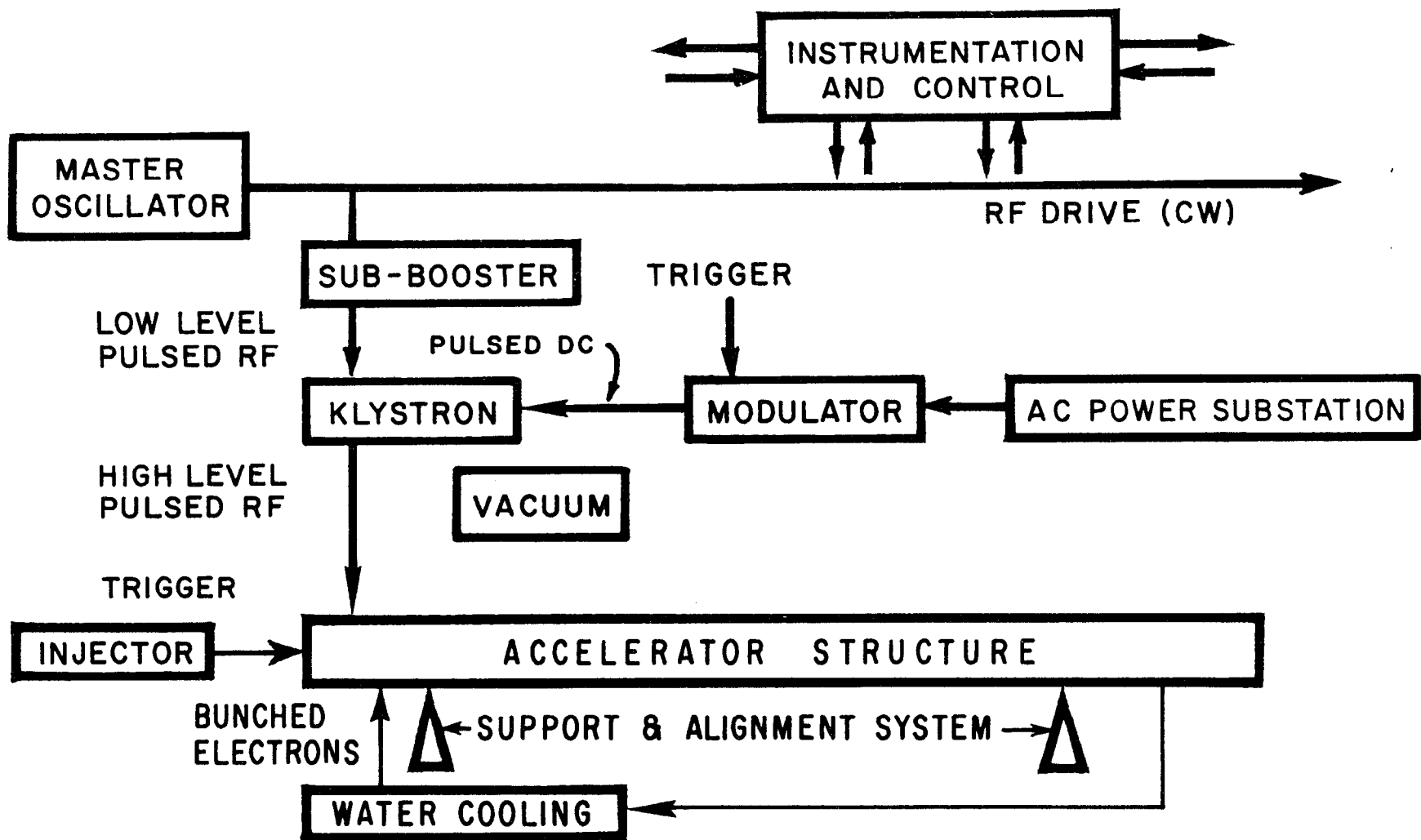


AP - Pulsed Steering Magnet  
 C - Collimator  
 B - Bending Magnet  
 PM - Pulsed Magnet

D - Beam Dump  
 Q - Quadrupole  
 SL - Energy Defining Slit  
 A - dc Steering Magnet

353-10-A

FIG. 4

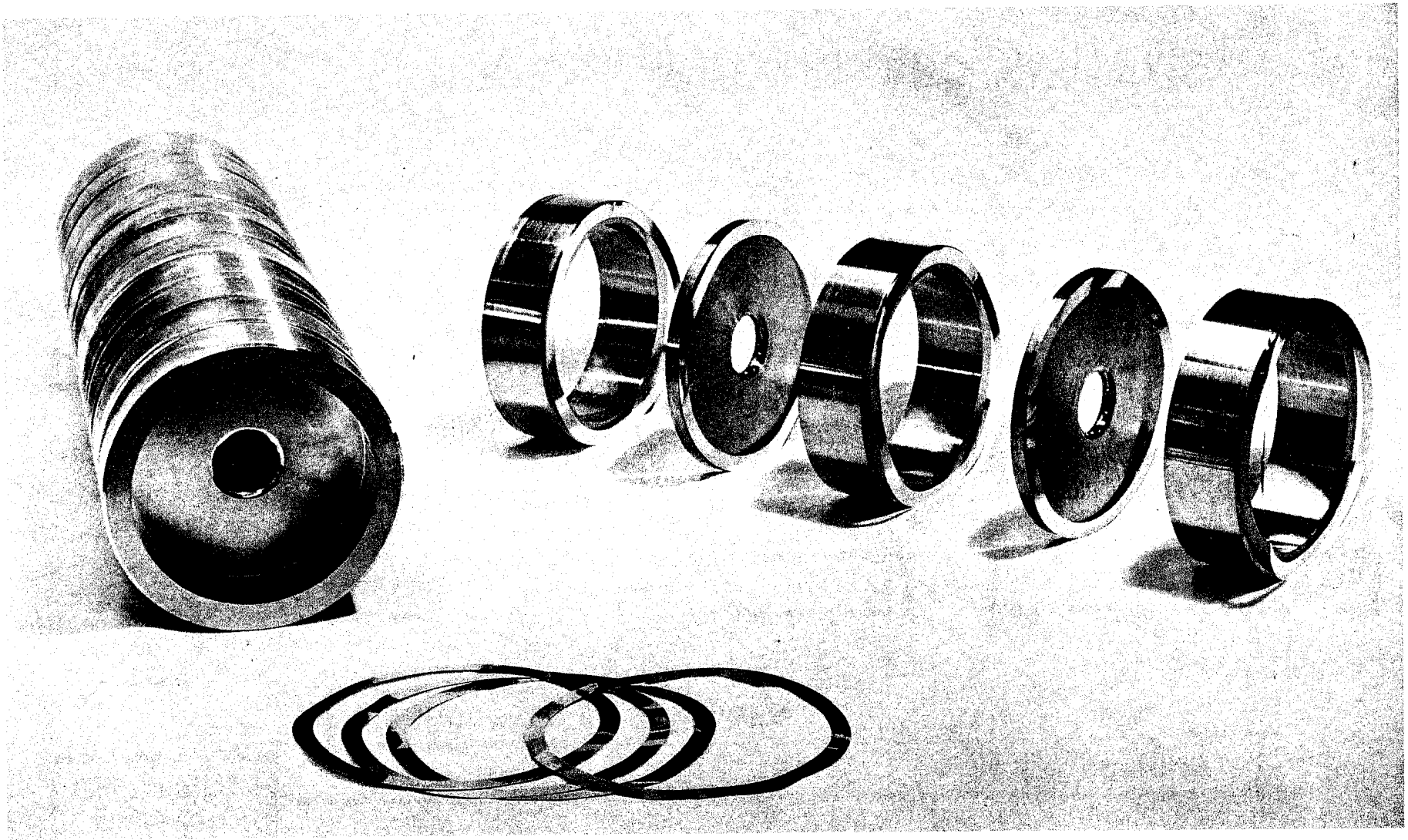


# ACCELERATOR COMPONENTS AND SYSTEMS

209-4-A

FIG. 5

*Slide 364*



631-2-A

FIG. 6



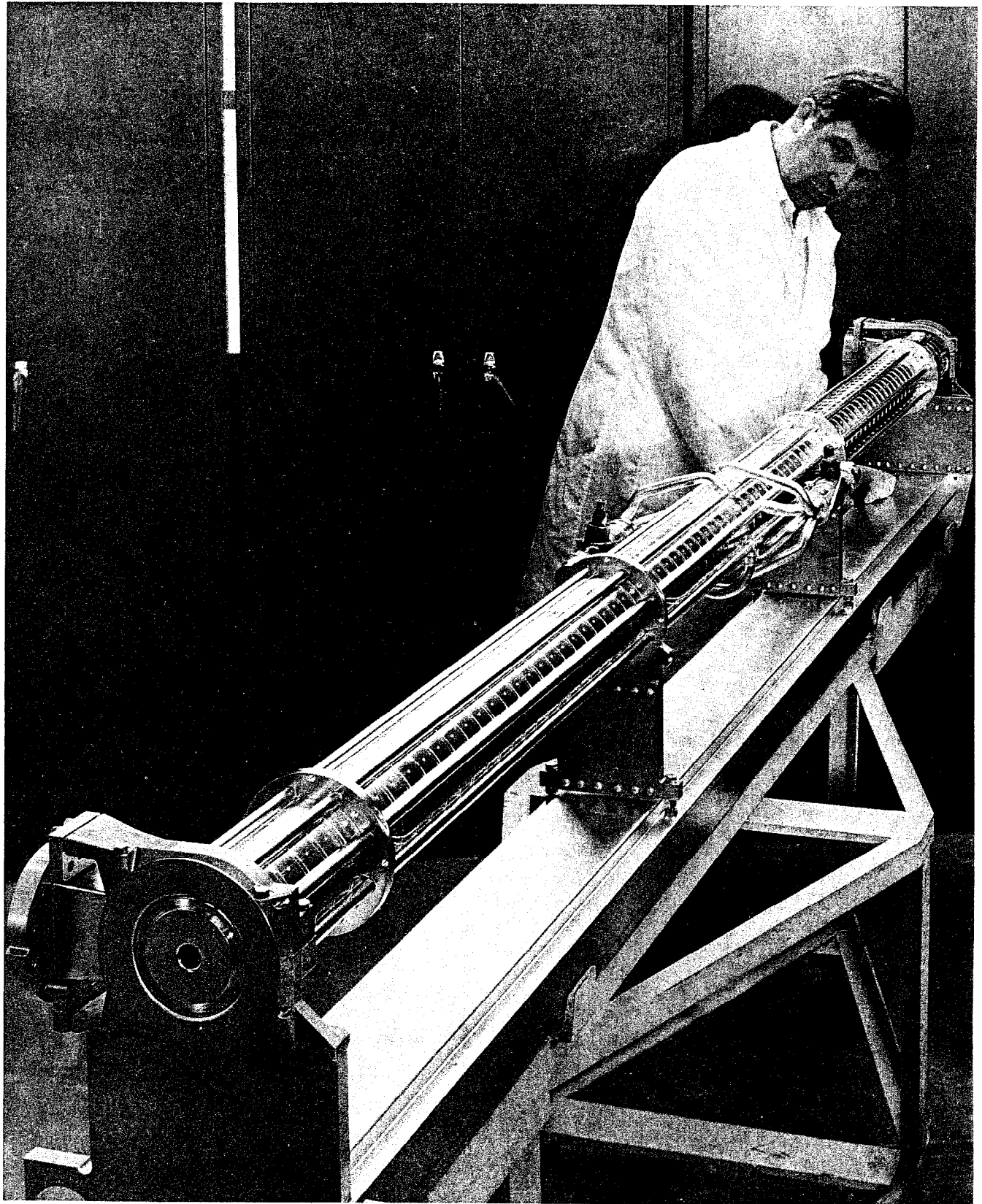
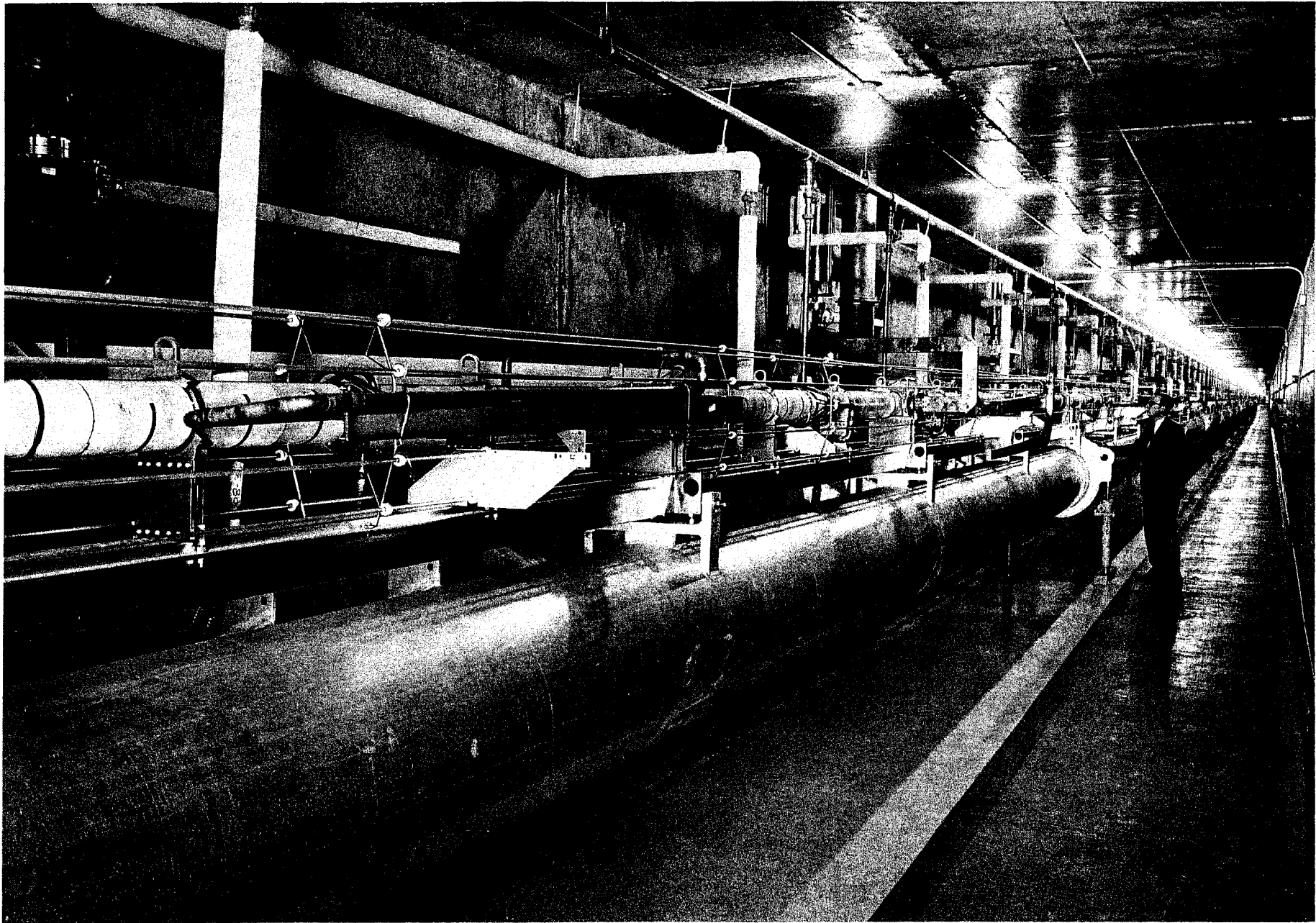


FIG. 7

593-5-A

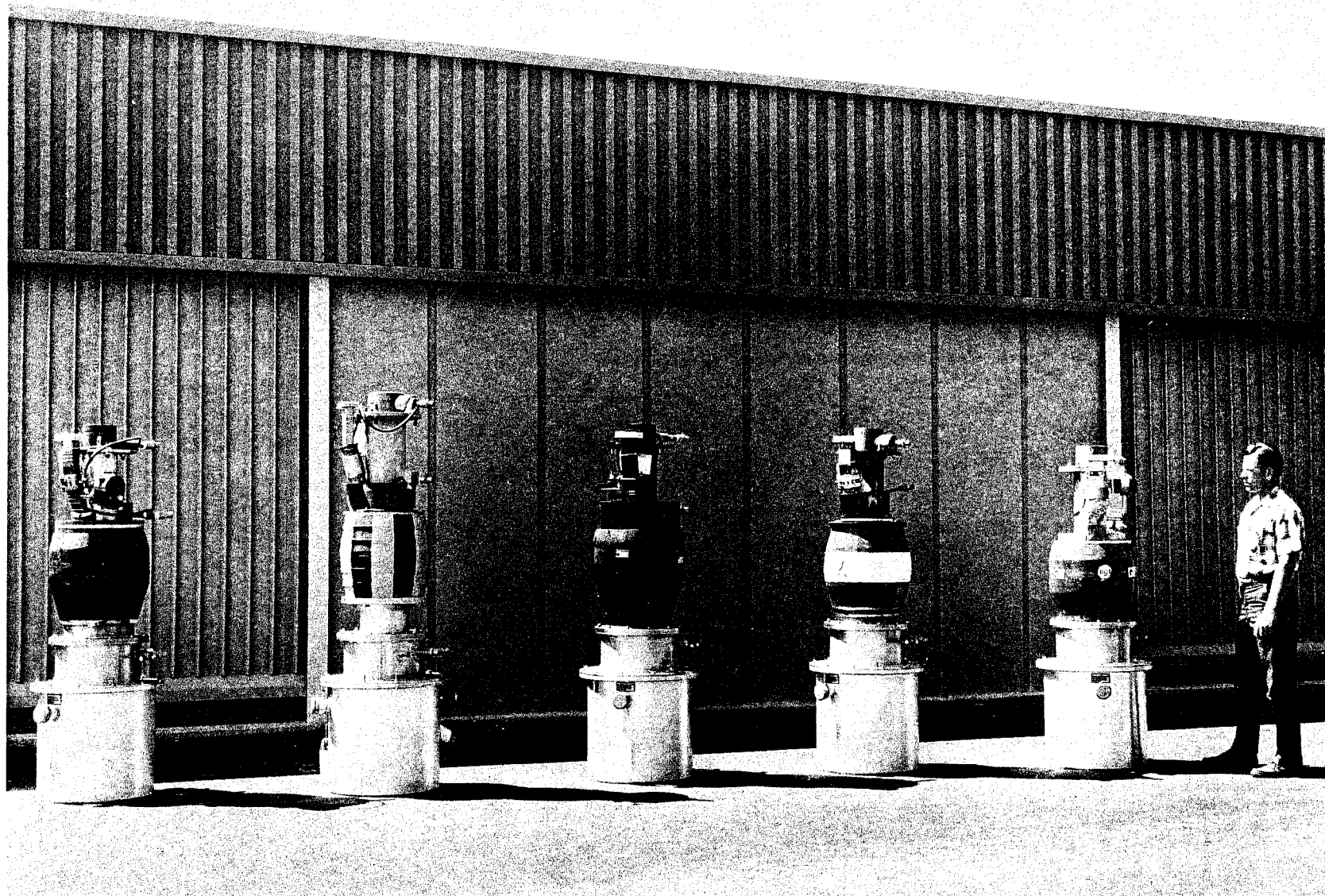
465

10114



631-1-A

FIG. 8

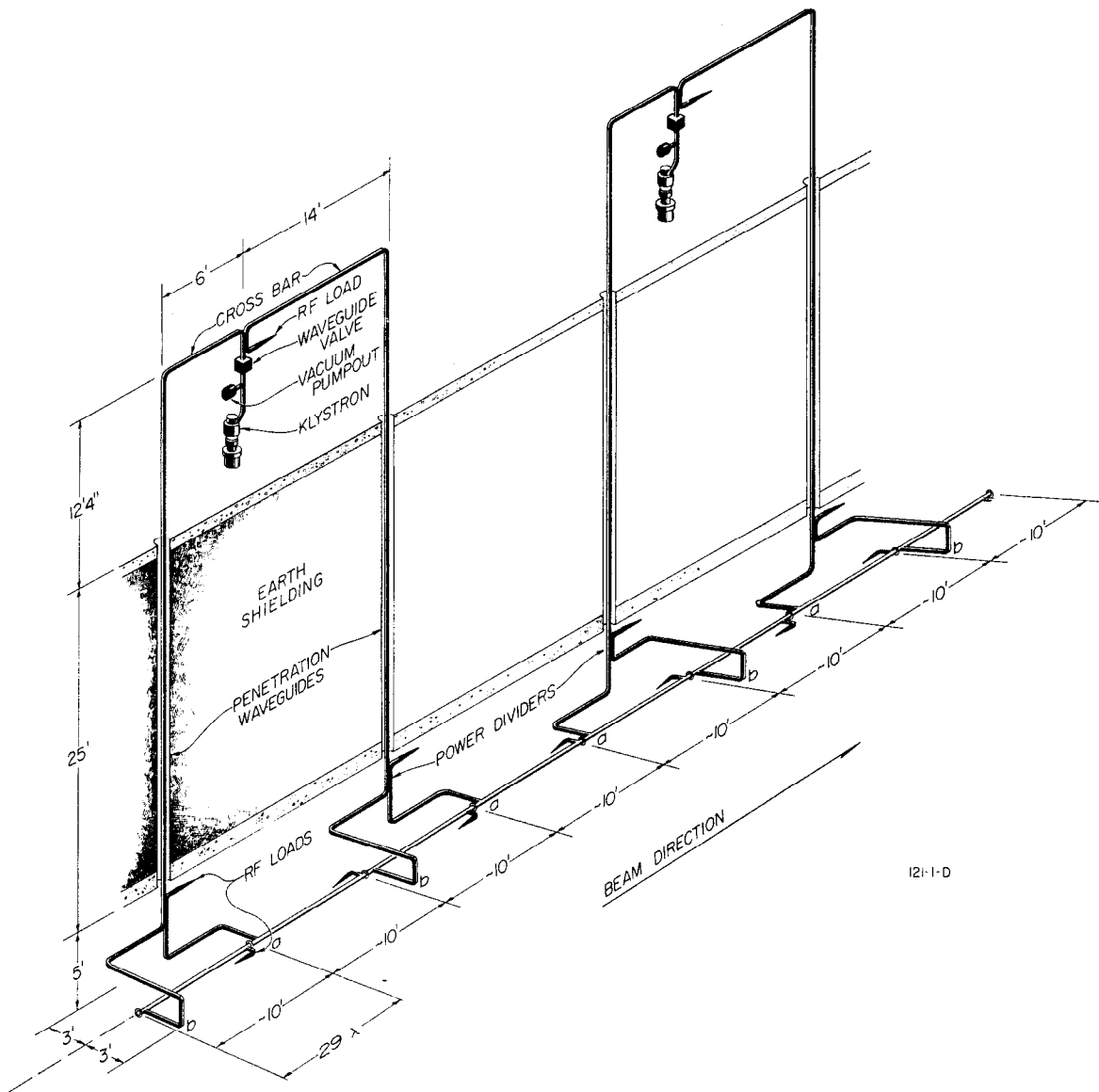


353-5-A

FIG. 9

*Slide 577*

*1/1/50*



121-1-D

FIG. 10

Sl 45  
M 1067

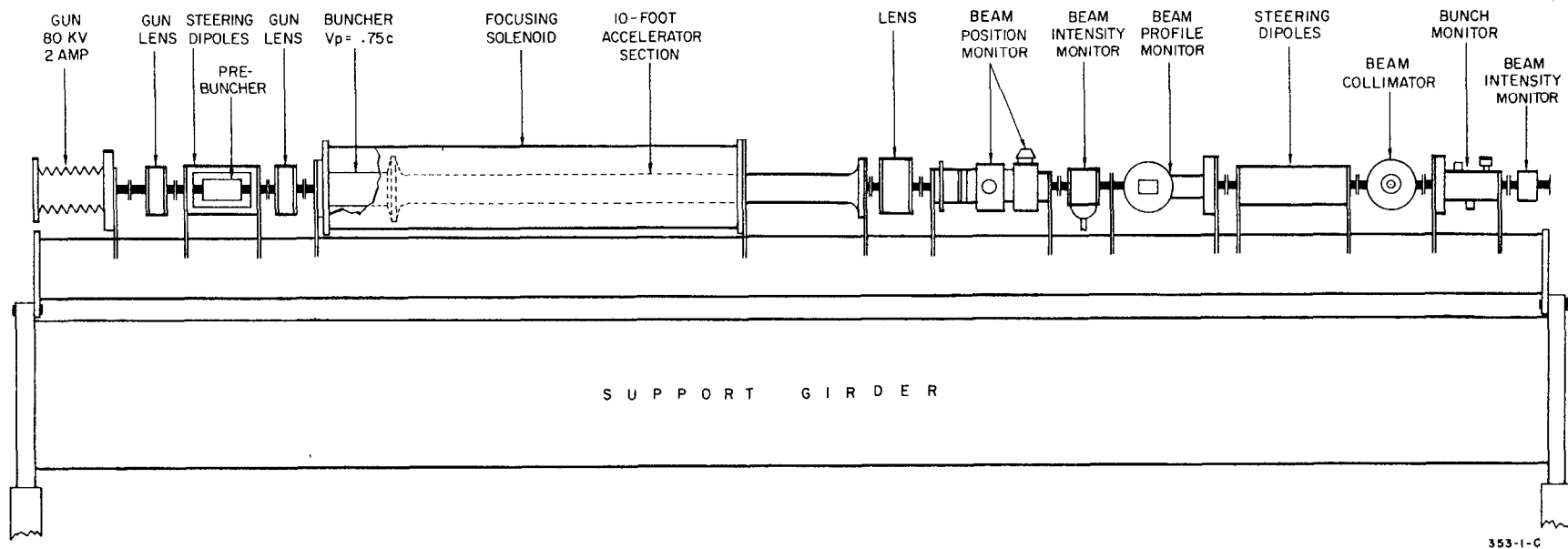


FIG. 11

✓  
 1951  
 M 1280-5

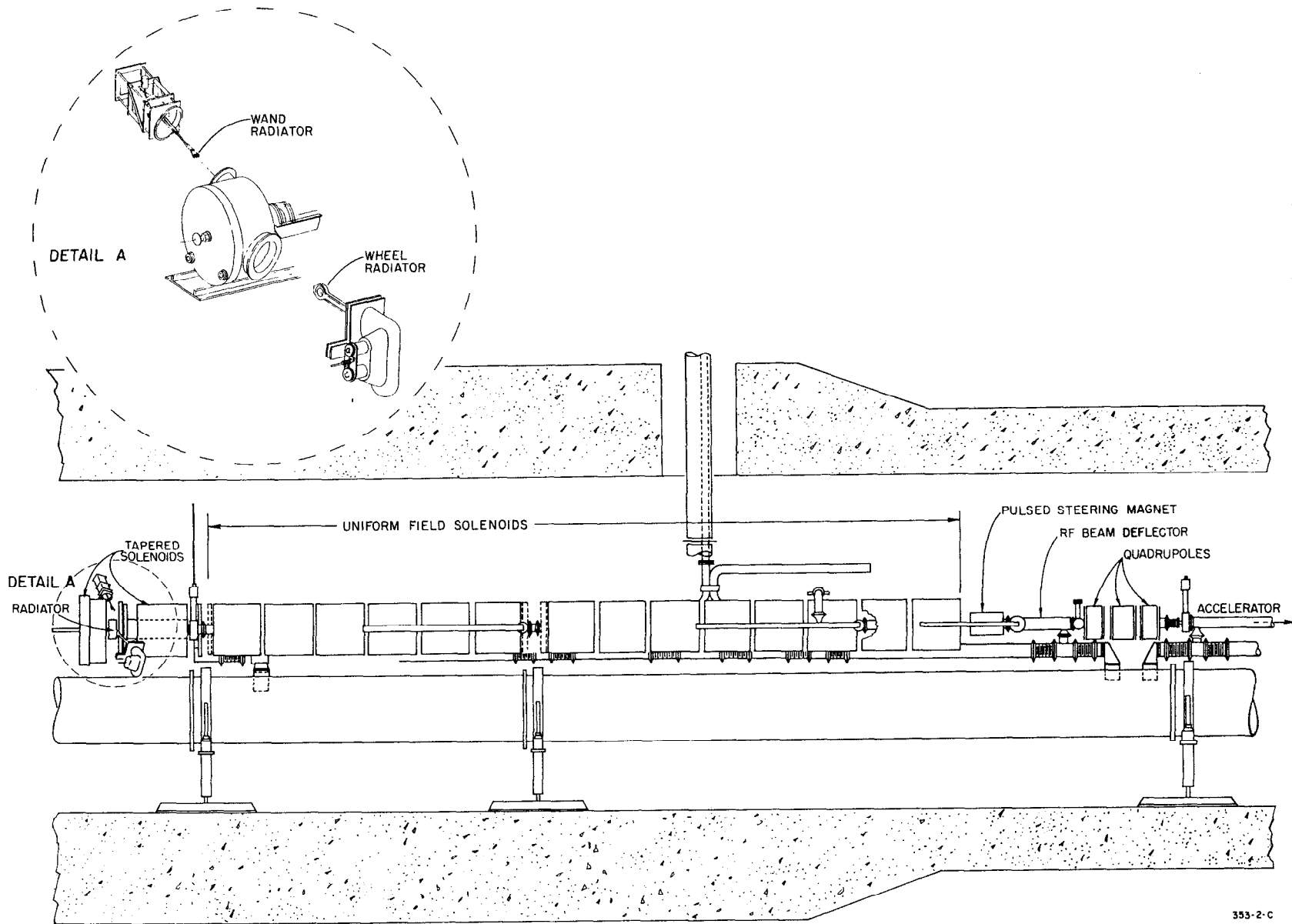


FIG. 12

SI 5000  
 10/10/50

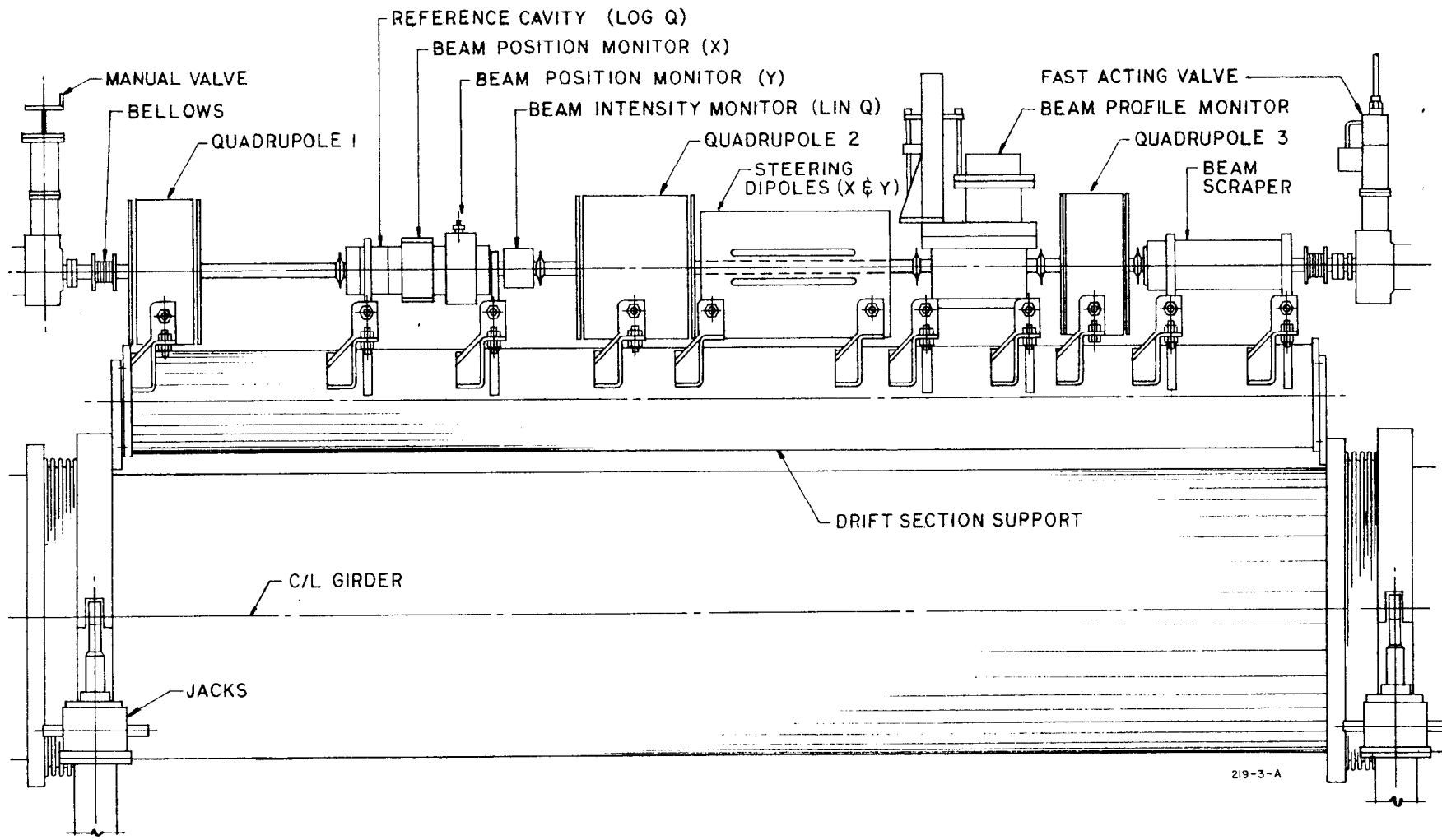
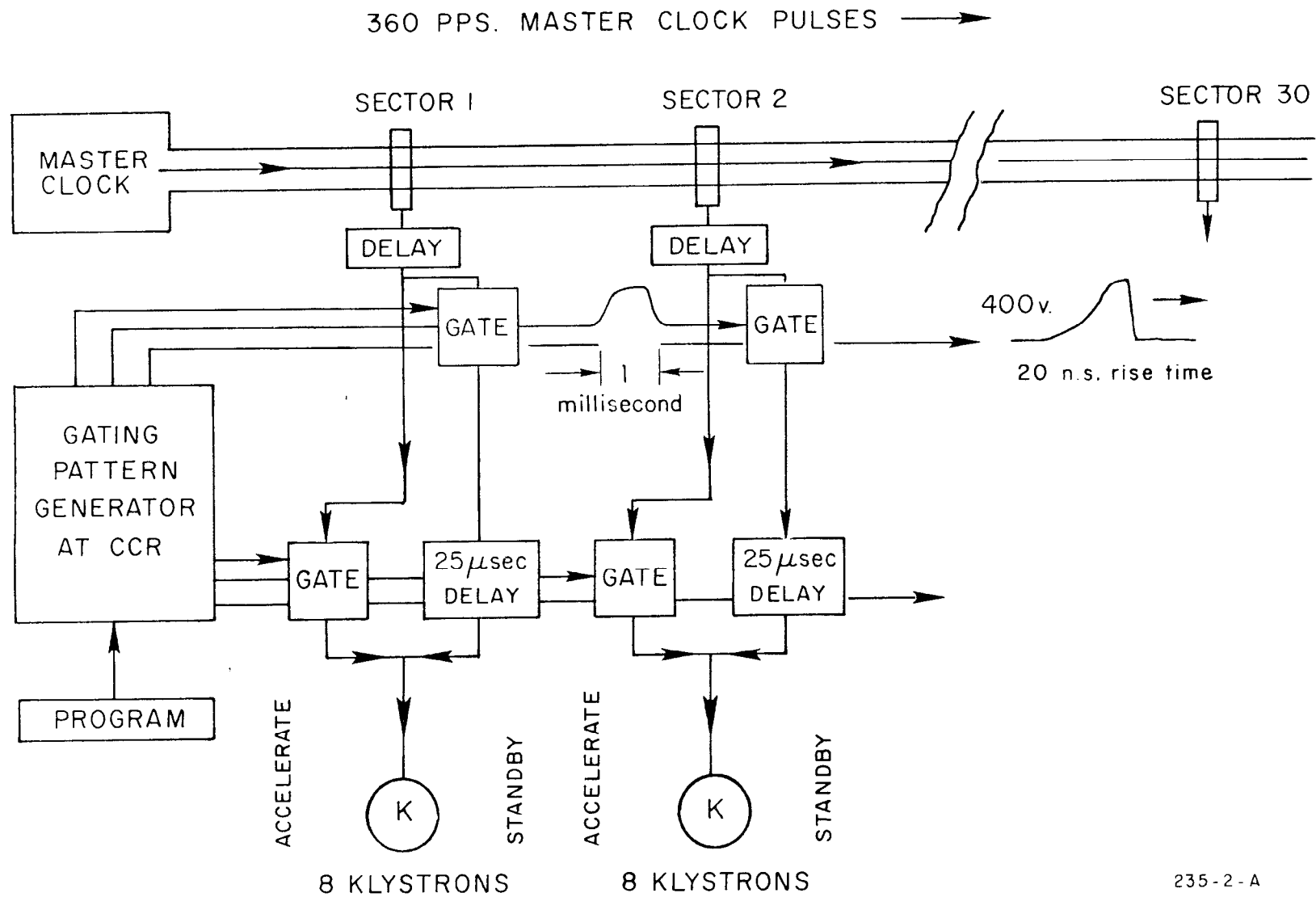


FIG. 13

SE 517

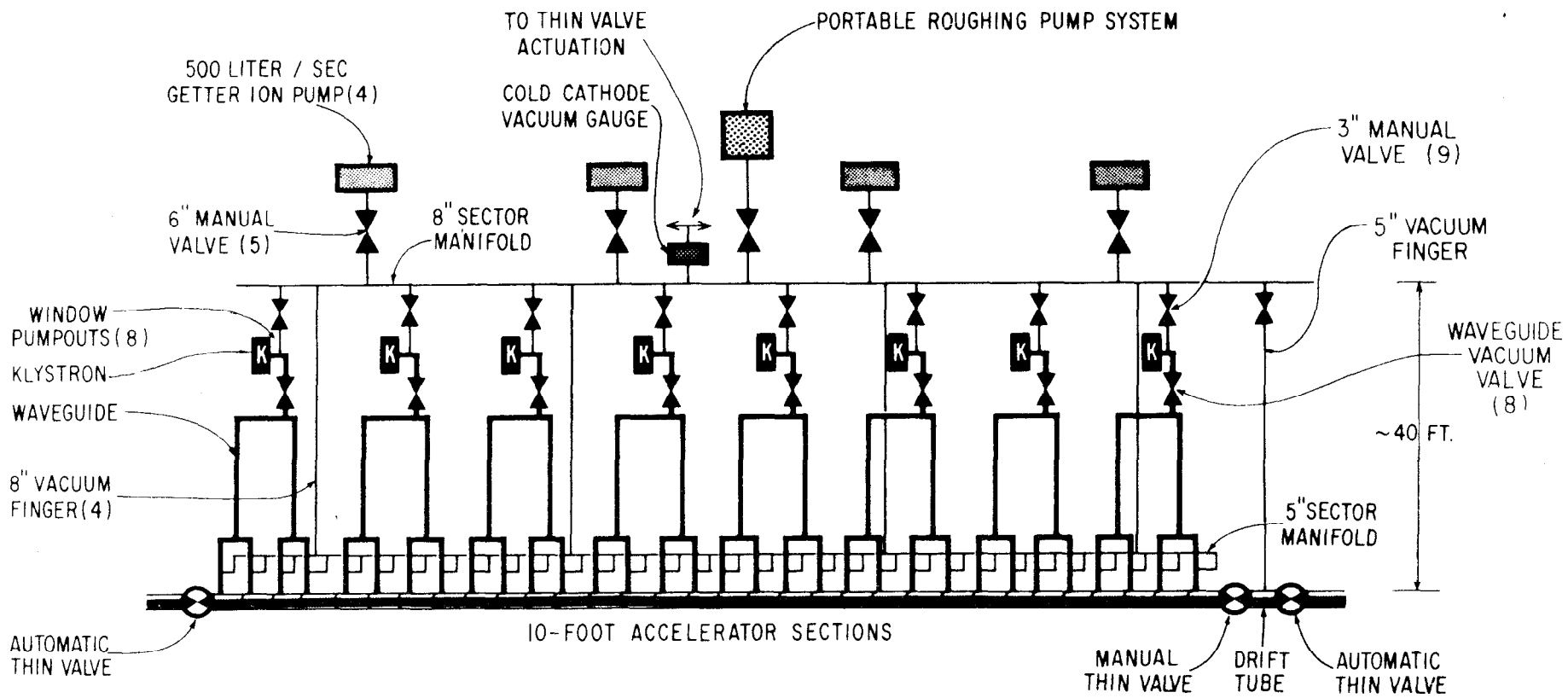
M 1726-10



235-2-A

FIG. 14





145-10-8

FIG. 15

Slide 401

M 1786-7 and

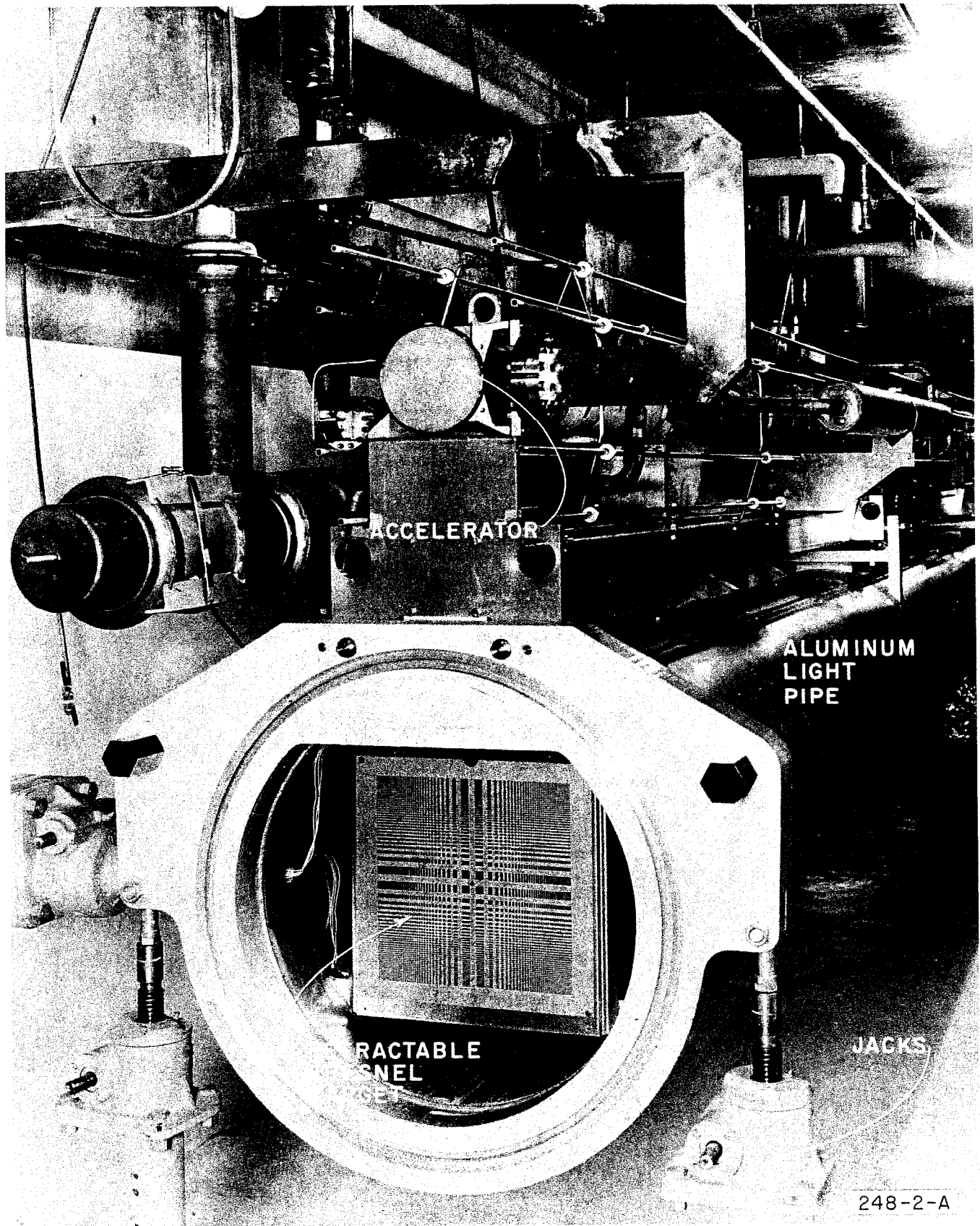
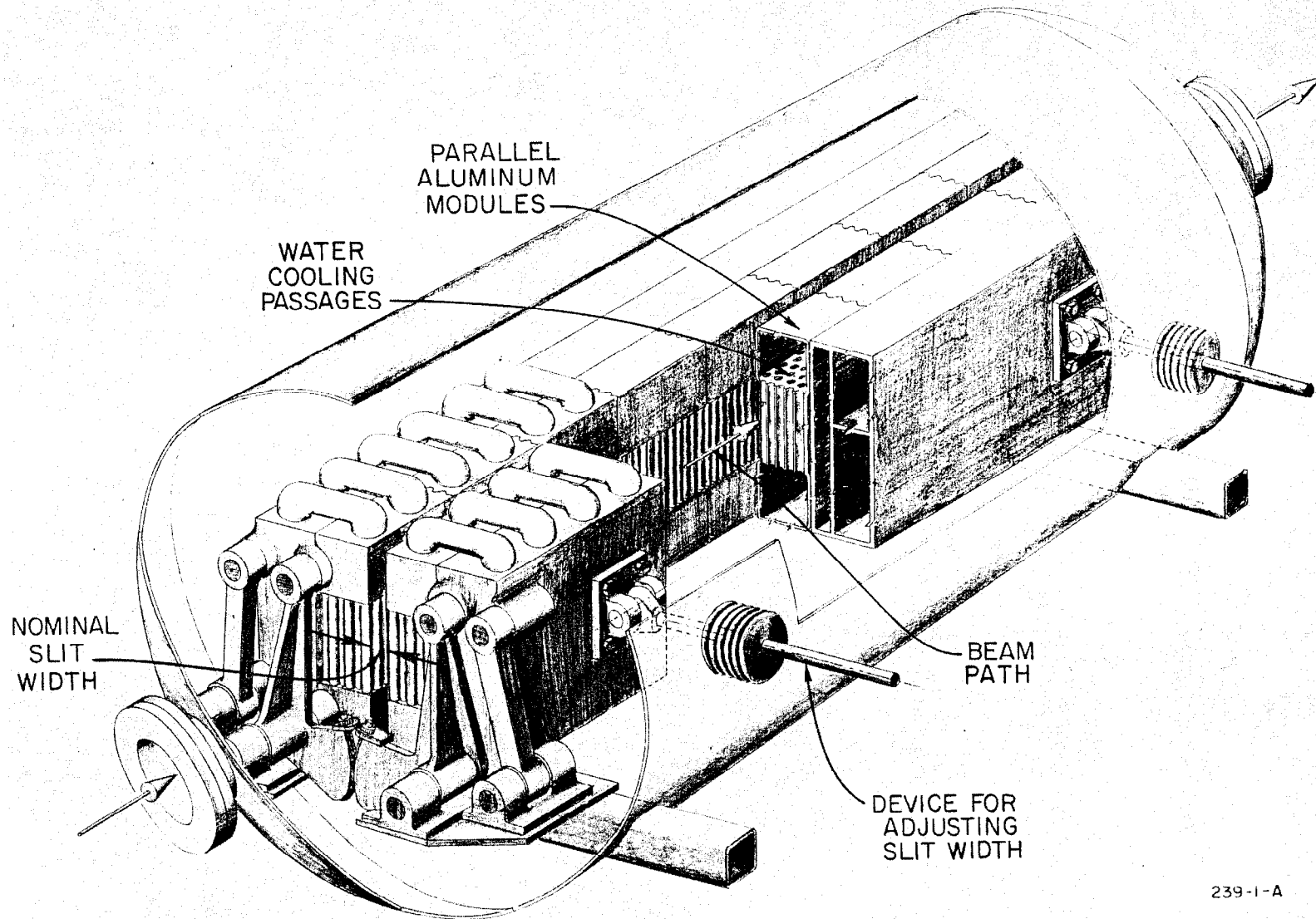


FIG. 16

m 1787



239-1-A

FIG. 17

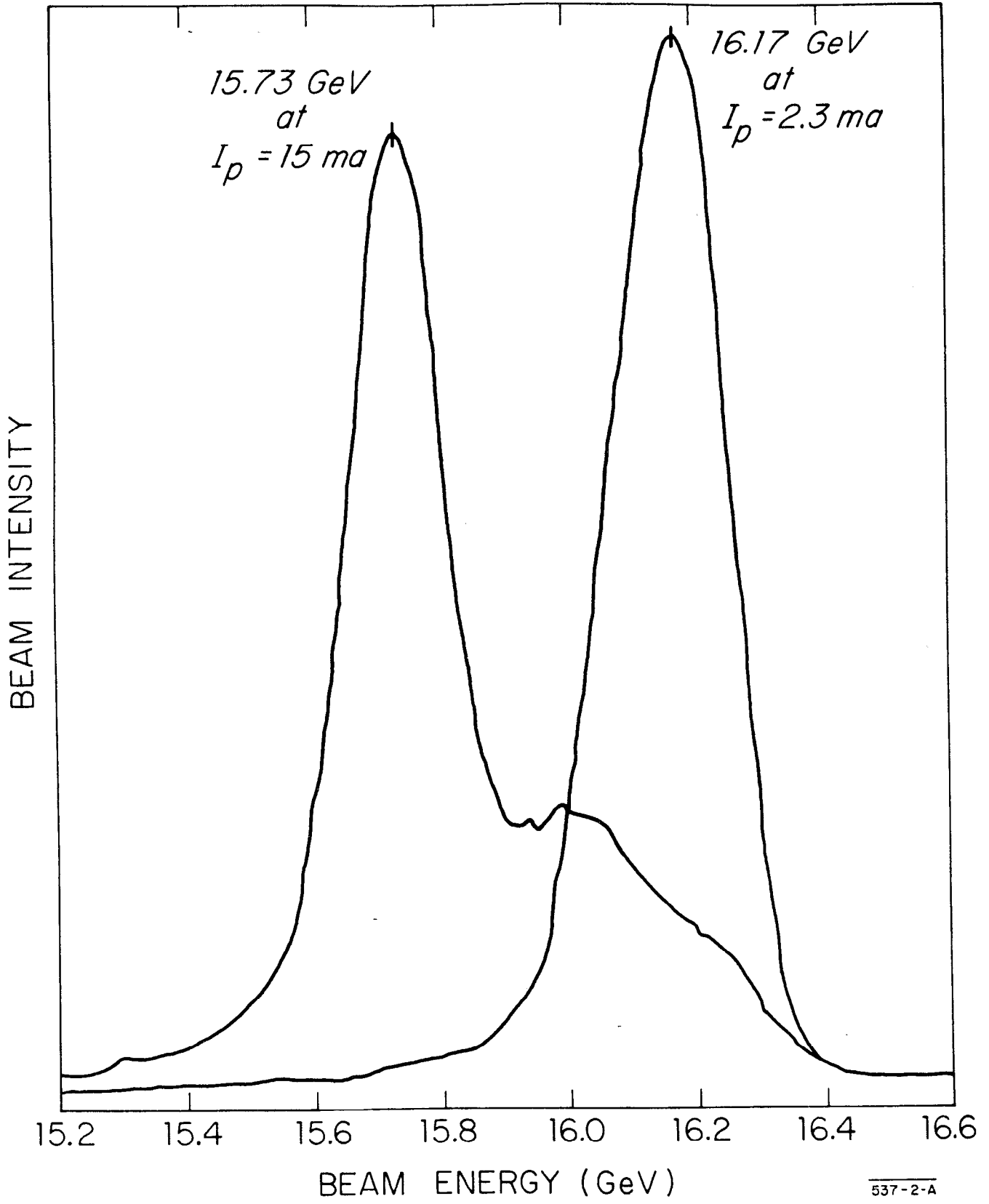


FIG. 18

10 20 30

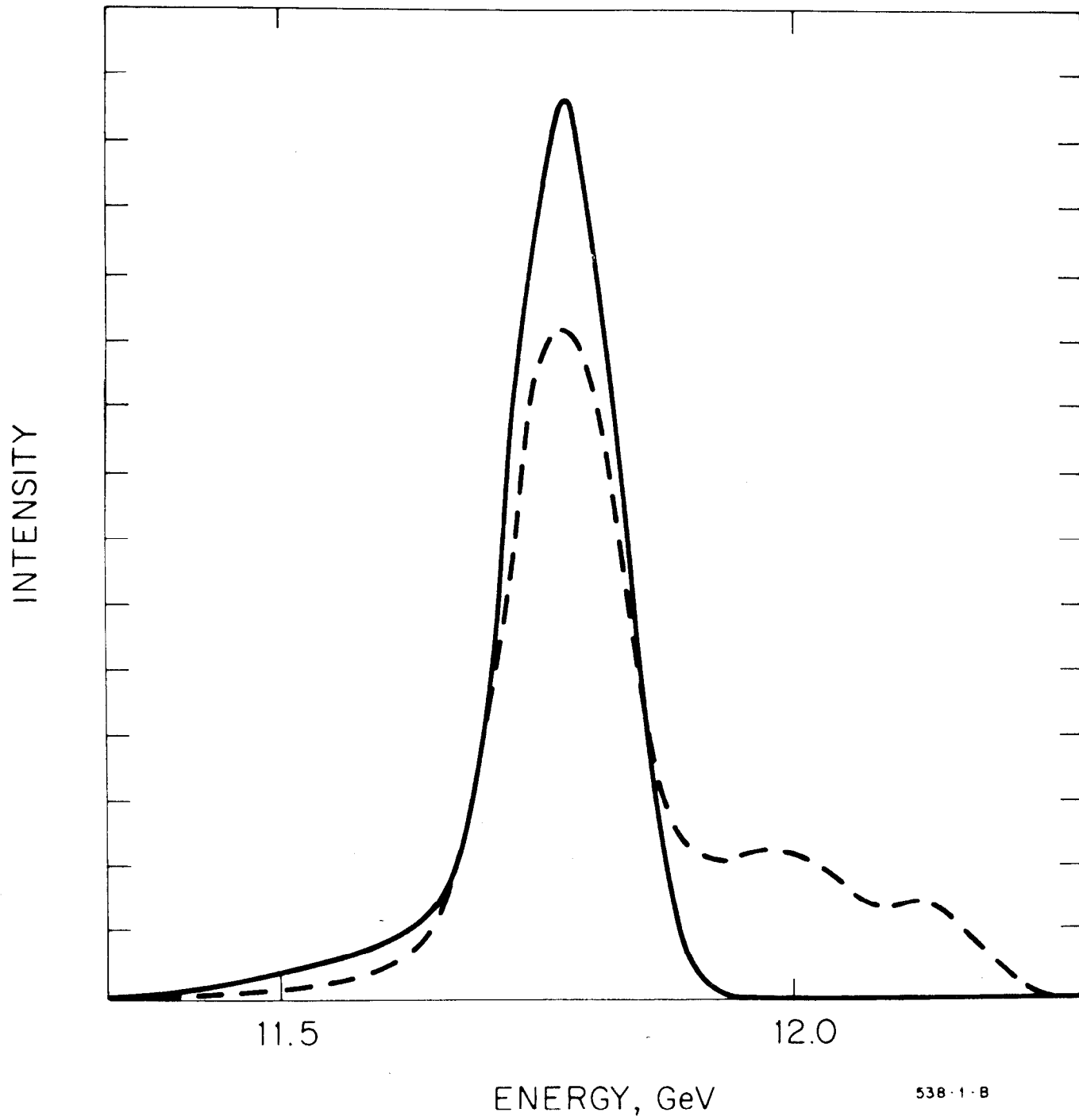
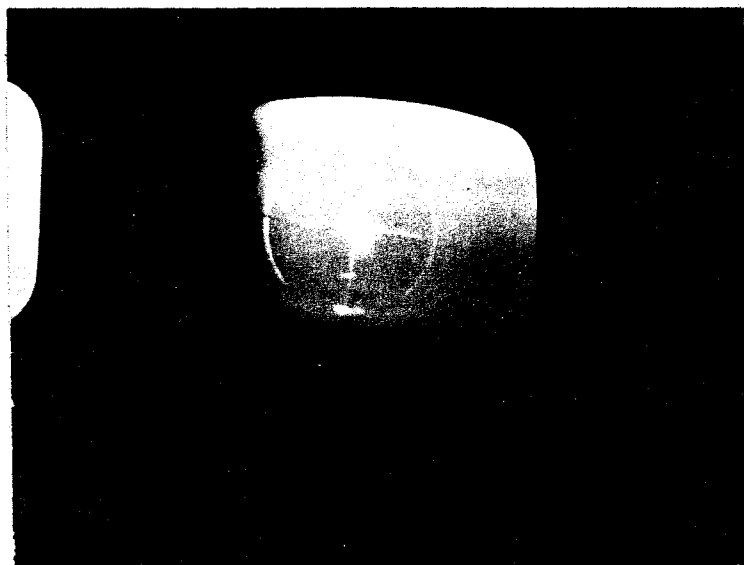


Fig. 19

252



CERENKOV CELL PR2.

VIEW OF FIRST 2-MILE BEAM CENTERED WITH BSY STEERING.

6:45 A.M.

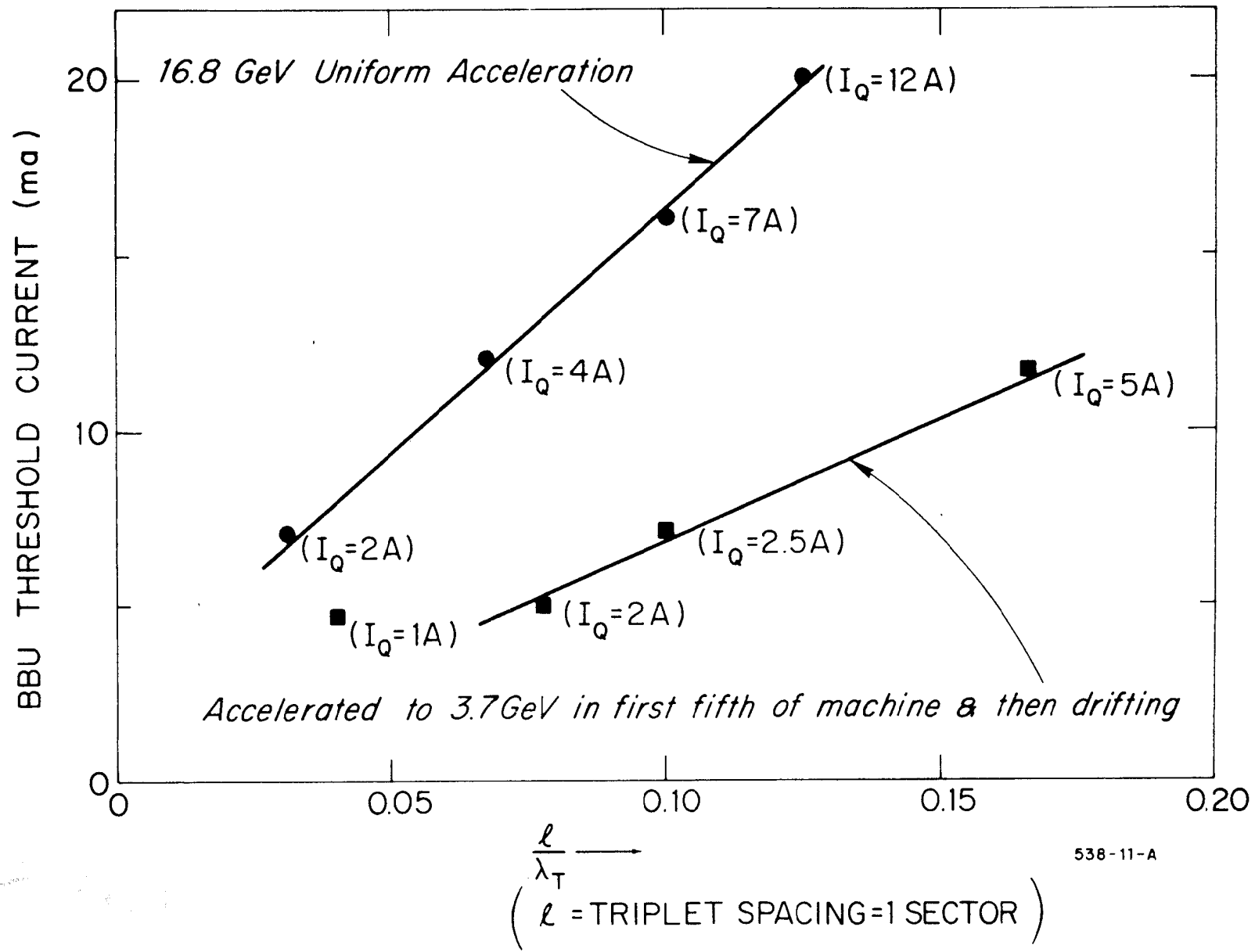
MAY 21, 1966

FIG. 20

631-3-A

*M 20-17*

*631-3-A*



538-11-A

FIG. 21